図❸ プラズマX線微小血管造影装置（文献9より改変）

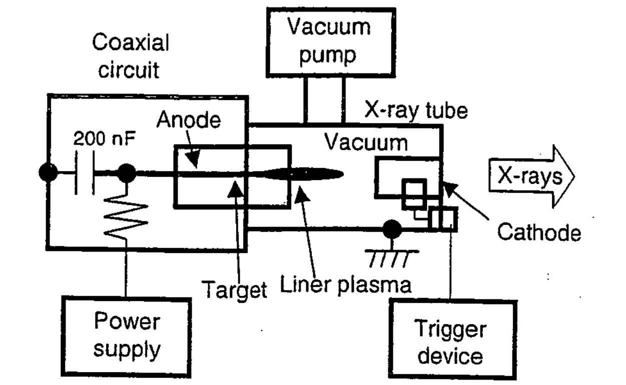

高電圧コンデンサーに約50～60V充電すると，陽極のターゲット金属が気化されプラズマを形成する。トリガ装置によりX線管内へ放電し，擬似単色X線を発生させる。

図❹ プラズマX線の発生原理（文献9より改変）

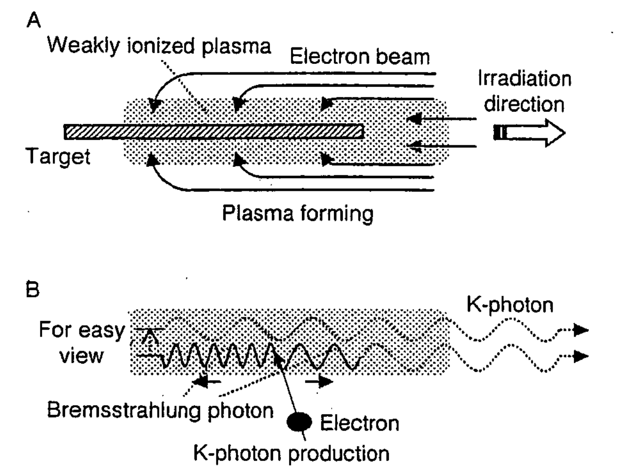

A. 高エネルギー放電により弱電離プラズマX線源を成長させ，線状に形成することにより制動X線を特性X線に変換する。
B. K系列線はL系列線と比較して，制動X線から特性X線への変換率が高い。

を計測した。X線発生装置から1mに検出器を設置し，管電圧70kV，管電流500mAで20秒照射した場合，0.547Sv（62.7R）であった。検査の撮影条件としては最低でも1検査あたり100R以下（3R/sec）を目標としており，妥当な線量と考えられる。また，X線発生装置から1mの距離にファントムを置き，50cm側方で散乱X線を検出した場合の散乱X線量は0.0225mSv（2.58mR）であった。放射線医療従事者の年間被曝量の限度は50mSvであり，許容範囲内と考えられる。本装置は，2004年3月に国立循環器病センターに設置され，医師主導のもと，臨床応用が開始される。

3．プラズマX線微小血管造影法

装置は高電圧電源，高電圧コンデンサー，プラズマX線管からなり，高電圧コンデンサーの容量を増すことによりX線の高輝度化が可能となる（図❸）。プラズマX線はシャープなK系列特性X線であり，その発生原理は高エネルギー放電により弱電離プラズマX線源を成長させ，線状に形成することにより制動X線を特性X線に変換する。特性X線はプラズマを容易に通過するので，高線量の疑似単色X線が発生する（図❹A）。さらに，K系列特性線は蛍光吸収率が高いので，L系列線と比較して制動X線から特性X線への変換率が高い（図❹B）。プラズマX線は金属ターゲットの種類により，特性X線のエネルギーを任意に選択することができる。例えば，セリウムを陽極に用いると約34keVの特性X線を得られ，ヨードのK吸収端である33keV直上のエネルギーを持つ擬似単色X線での撮影が可能となる[9]。

Ⅱ．微小血管の画像による評価

1．正常血管と再生血管の比較

Takeshitaらは，放射光微小血管造影装置を用い，ラットの大腿動脈を結紮した後の再生血管と結紮処置をしていないコントロールの血管性状を比較した[10]。結紮してから4週後に血管撮影をした結果，線状とらせん状の2種類の血管が存在したが，コントロールでは線状の血管のみであり，らせん状の血管は観察されなかった。このことから，再生される血管には線状とらせん状の2種類の構造を持つ血管があるが，線状の血管は既存の血管であった可能性もあると示唆した。しかし，らせん状の血管はコントロールでは観察されないため，少なくとも虚血により再生した結果で生じた血管であるとしている。また，血管内皮依存性の血管拡張薬であるアセチルコリンを投与した場合，線状の血管は拡張するものの，らせん状の血管は拡張しなかった。さらに，血管内皮増殖因子である

Acta Crystallographica Section F
Structural Biology and Crystallization Communications
ISSN 1744-3091

Crystallization and preliminary crystallographic analysis of the human calcineurin homologous protein CHP2 bound to the cytoplasmic region of the Na^+/H^+ exchanger NHE1

Youssef Ben Ammar,[a] Soichi Takeda,[b] Mitsuaki Sugawara,[c] Masashi Miyano,[c] Hidezo Mori[b] and Shigeo Wakabayashi[a]*

[a]Department of Molecular Physiology, National Cardiovascular Center Research Institute, Fujishiro-dai 5-7-1, Suita, Osaka 565-8565, Japan, [b]Department of Cardiac Physiology, National Cardiovascular Center Research Institute, Fujishiro-dai 5-7-1, Suita, Osaka 565-8565, Japan, and [c]Structural Biophysics Laboratory, RIKEN Harima Institute at SPring-8, Kouto, Mikazuki, Sayo, Hyogo 679-5148, Japan

Correspondence e-mail: wak@ri.ncvc.go.jp

Received 18 August 2005
Accepted 27 September 2005
Online 30 September 2005

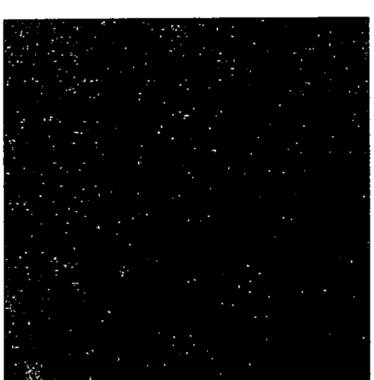

Calcineurin homologous protein (CHP) is a Ca^{2+}-binding protein that directly interacts with and regulates the activity of all plasma-membrane Na^+/H^+-exchanger (NHE) family members. In contrast to the ubiquitous isoform CHP1, CHP2 is highly expressed in cancer cells. To understand the regulatory mechanism of NHE1 by CHP2, the complex CHP2–NHE1 (amino acids 503–545) has been crystallized by the sitting-drop vapour-diffusion method using PEG 3350 as precipitant. The crystals diffract to 2.7 Å and belong to a tetragonal space group, with unit-cell parameters $a = b = 49.96$, $c = 103.20$ Å.

1. Introduction

The Na^+/H^+ exchangers (NHEs) are electroneutral transporters that catalyze the countertransport of Na^+ and H^+ through the plasma membrane and other intracellular organellar membranes in various animal species (Wakabayashi *et al.*, 1997; Orlowski & Grinstein, 2004). Nine different NHE isoforms (NHE1–NHE9) have been identified in mammalian tissues. Although they have been shown to exhibit similar membrane topology, these isoforms are thought to play different roles in various tissues (Counillon & Pouysségur, 2000; Orlowski & Grinstein, 2004). The isoform NHE1 is ubiquitously expressed in all tissues and cell types and plays a major role in maintaining intracellular pH and cell-volume homoeostasis (Putney *et al.*, 2002). The activity of NHE1 is controlled by various extrinsic factors, including growth factors, hormones and mechanical stimuli (Wakabayashi *et al.*, 1997; Counillon & Pouysségur, 2000; Orlowski & Grinstein, 2004). NHE1 is regulated by a variety of signalling molecules including calcineurin B homologous protein (CHP; Lin & Barber, 1996; Pang *et al.*, 2001) and Ca^{2+}/calmodulin (Bertrand *et al.*, 1994; Wakabayashi *et al.*, 1994). Despite intensive studies on NHE1 and its regulation, structural information is extremely limited, especially for the cytoplasmic C-terminal domain which contains most of the binding domains for the regulatory proteins.

CHP was initially identified as a protein (p22) involved in vesicular transport (Barroso *et al.*, 1996) and also as a molecule that interacts with NHE (Lin & Barber, 1996). CHP has also been reported to be involved in various cell functions, such as inhibition of calcineurin phosphatase activity (Lin *et al.*, 1999) and interaction with microtubules (Timm *et al.*, 1999), DRAK2 (death-associated protein kinase-related apoptosis-inducing protein kinase 2; Matsumoto *et al.*, 2001) and KIF1Bβ2 (kinesin family 1Bb2; Nakamura *et al.*, 2002). We have previously reported that CHP is an essential cofactor for supporting the physiological activity of the Na^+/H^+ exchanger by interacting with its juxtamembrane cytoplasmic domain (Pang *et al.*, 2001). Furthermore, we demonstrated that in contrast to the ubiquitous CHP1 isoform, CHP2 (61% amino-acid identity with CHP1) is highly expressed in malignantly transformed cells and may be involved in maintaining the high intracellular pH (pH_i) in cancer cells (Pang *et al.*, 2002). NHE1 mutants lacking the CHP-binding region (amino acids 515–530) exhibited low exchange activity (5–10% of the wild-type level; Pang *et al.*, 2001), suggesting that this region is essential for normal exchange activity of NHE1. This region with bound CHP would therefore function as a key structure maintaining the physiologically active conformation of NHE1 (Pang *et al.*, 2001).

Consequently, more detailed structural information including the crystal structure of CHP complexed with its binding domain is of great importance to reveal the mechanism by which CHP is involved in this important regulation pathway of NHE1.

Here, we report the first crystallization and preliminary crystallographic studies of the human CHP2 complexed with the C-terminal cytoplasmic region (amino acids 503–545) of NHE1. Hereafter, the protein complex is referred to as CHP2–NHE1-peptide.

2. Materials and methods

2.1. Protein expression and purification

Human CHP2 cDNA (GenBank accession No. AF146019) corresponding to amino-acid residues 1–196 cloned into pET11 vector (Novagen) as a fusion protein with a C-terminal His_6 tag was coexpressed in *Escherichia coli* (BL21-Star; Invitrogen) with the human cDNA encoding the cytoplasmic binding-domain region of NHE1 peptide cloned into pET24 vector (Novagen). Six histidine residues were inserted after Lys196 of CHP2, while a stop codon was incorporated just after the sequence coding for the NHE1 peptide to eliminate the His_6 tag from the vector. Using this coexpression system, as also described previously for CHP1 (Pang *et al.*, 2004), we were able to obtain CHP2 in a complex form with its binding domain of NHE1. Cells were cultured in 2×YT medium containing 100 µg ml^{-1} ampicillin and 100 µg ml^{-1} kanamycin at 310 K. At an optical density of 0.6 at 600 nm, protein expression was induced by the addition of IPTG to a final concentration of 1 m*M* and cells were grown overnight at 291 K. The cells were harvested and resuspended in PBS buffer containing 1 m*M* phenylmethylsulfonyl fluoride (PMSF) and disrupted by sonication at 277 K. After centrifugation at 277 K, the supernatant containing the complex CHP2–NHE1-peptide was applied onto an Ni–NTA agarose affinity column (Invitrogen) equilibrated with PBS buffer. The column was washed with buffer *A* (20 m*M* sodium phosphate, 500 m*M* NaCl and 2 *M* KCl pH 6.0), buffer *B* (20 m*M* sodium phosphate and 500 m*M* NaCl pH 4.7) and then buffer *C* (20 m*M* sodium phosphate and 500 m*M* NaCl pH 6.0). The adsorbed protein complex was eluted with buffer *C* containing 500 m*M* imidazole, dialyzed overnight against buffer *D* (20 m*M* Tris–HCl pH 8.5) and further purified using a DEAE-Sepharose column (HiTrap DEAE FF 5 ml; Amersham Biosciences) eluted with a gradient from 0 to 1 *M* NaCl in 20 m*M* Tris–HCl buffer pH 8.5. A final purification step was carried out using gel-filtration chromatography (Superdex 200; Amersham Bioscience). The gel-filtration column was eluted with a buffer solution containing 100 m*M* NaCl and 20 m*M* Tris–HCl pH 7.5. The fraction containing CHP2–NHE1-peptide was pooled, dialyzed against 20 m*M* Tris–HCl pH 7.5, concentrated (20–25 mg ml^{-1}) using Amicon Ultra (Millipore) and subjected to crystallization without removing the His_6 tag.

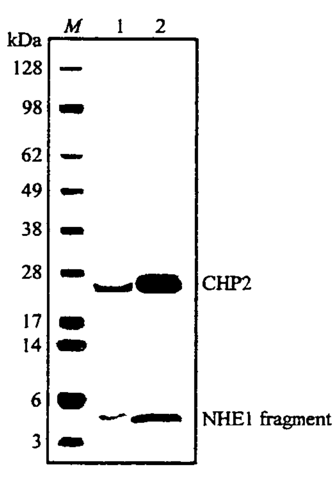

Figure 1
Polyacrylamide gel-electrophoresis pattern of the complex CHP2–NHE1-peptide. Crystals were collected and washed with the cryoprotectant solution. Collected crystals and 10 µg of the purified complex were applied to 4–12% gradient gel for lanes 1 and 2, respectively. Proteins were stained with Coomassie Brilliant Blue.

2.2. Crystallization

Preliminary screening of crystallization conditions was performed using various commercial kits (Hampton Research Crystal Screen kits, Emerald BioSystems Screen kits, Sigma–Aldrich Crystallization kits) and carried out using the sitting-drop vapour-diffusion method at 293, 287 and 277 K. 1 µl aliquots of protein-complex solution (20–25 mg ml^{-1}) were mixed with 1 µl reservoir solution to form the droplet, which was equilibrated against 100 µl reservoir solution. The initial screening, involving about 1440 individual trials, was unsuccessful. Additives from Hampton Research were used together with the above screening kits in a second trial involving about 4320 individual trials and very small and thin needle-shape crystals were finally obtained with a crystallization solution containing 200 m*M* ammonium acetate, 100 m*M* Bis-Tris pH 5.5, 25%(*w*/*v*) polyethylene glycol 3350 (PEG 3350) and 5 m*M* yttrium chloride as an additive at 277 K. Refinement of the crystallization conditions to 200 m*M* ammonium acetate, 100 m*M* Bis-Tris pH 5.5, 25%(*w*/*v*) PEG 3350 and 10 m*M* yttrium chloride at 293 K improved the size of the crystals. The resultant crystals are mostly in clusters, with the occasional appearance of single crystals. Single crystals or dissected parts from the clusters were used for data collection.

2.3. Crystallographic data collection

Prior to data collection, single crystals were soaked in a solution containing 200 m*M* ammonium acetate, 100 m*M* Bis-Tris pH 5.5, 35%(*w*/*v*) PEG 3350 and 10 m*M* yttrium chloride and flash-frozen under a nitrogen flow at 100 K. The crystals were evaluated in-house with Cu *Kα* radiation (λ = 1.5418 Å) generated by an RA-Micro 7 rotating-anode X-ray generator with R-AXIS VII imaging-plate detector (Rigaku). High-resolution data sets were collected using an

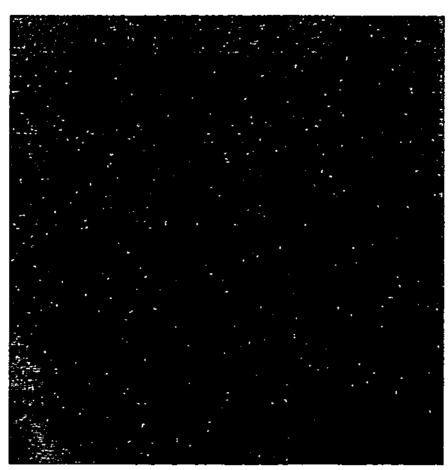

Figure 2
Crystal of human CHP2–NHE1-peptide as grown by the sitting-drop method. The scale bar indicates 0.1 mm.

Table 1
Data-collection statistics.

Values in parentheses are for the highest resolution shell (2.8–2.7 Å).

X-ray source	SPring-8 BL41XU
Space group	$P4_1$ or $P4_3$
Unit-cell parameters (Å, °)	$a = b = 49.96$, $c = 103.20$, $\alpha = \beta = \gamma = 90$
Wavelength (Å)	1.0000
Resolution range (Å)	50.00–2.70 (2.80–2.70)
Total reflections	26984
Unique reflections	6807
R_{merge}† (%)	4.8 (25.1)
Completeness (%)	97.3 (83.1)
$\langle I/\sigma(I)\rangle$	17.3 (4.5)
Redundancy	4.0 (3.1)
Crystal mosaicity (°)	0.458

† $R_{merge} = \sum_{hkl}\sum_i |I_i(hkl) - \langle I(hkl)\rangle| / \sum_{hkl}\sum_i I_i(hkl)$, where $I_i(hkl)$ is the ith intensity measurement of reflection hkl and $\langle I(hkl)\rangle$ is its average.

ADSC Quantum 315 CCD detector installed on the BL41XU beamline at SPring-8. The data collection was performed at a wavelength of 1.000 Å over a total range of 180°, with individual frames of 1° and an exposure time of 4 s. The crystal-to-detector distance was 350 mm. The collected images were processed using *HKL2000* (Otwinowski & Minor, 1997).

3. Results and discussion

CHP is an important regulatory factor that maintains the physiologically active conformation of NHE1. In this study, in order to clarify the regulatory mechanism of NHE1 by CHP, we coexpressed CHP2 and its binding domain in NHE1 (amino acids 503–545) in *E. coli* and crystallized the complex. Firstly, we confirmed that the purified complex CHP2–NHE1-peptide was retained as a single peak on gel-filtration chromatography, indicating that the stable complex exists as a monomer (M_r = 28 000) in solution. In addition, using a 4–12% polyacrylamide gradient gel we confirmed that the purity of the complex is suitable for crystallization assay and that the purified sample contained equimolar amounts (1:1 molar ratio) of CHP2 and NHE1-peptide (Fig. 1).

Crystals suitable for X-ray crystallographic analysis were obtained within 2–3 d at 293 K using the sitting-drop vapour-diffusion method (Fig. 2). A previous attempt to collect crystallographic data at beamline BL44B2 (SPring-8) gave a maximum resolution of 3.0 Å owing to the small size of crystals. To obtain higher resolution data, we used the undulator beamline BL41XU. Crystals diffracted to 2.5 Å resolution along the *c* axis of the crystal, but the data set was only qualitatively useful to 2.7 Å because of anisotropic diffraction.

The tetragonal crystal of CHP2–NHE1-peptide was determined to be $P4_1$ or $P4_3$, with unit-cell parameters $a = b = 49.96$, $c = 103.20$ Å. Assuming the presence of one CHP2–NHE1-peptide complex molecule in the asymmetric unit, the Matthews coefficient V_M was calculated to be 2.5 Å^3 Da^{-1}, indicating a solvent content of approximately 49.5% in the unit cell. These values are within the typical range for protein crystals (Matthews, 1968).

The native data set has 6807 unique reflections, giving a data-set completeness of 97.3% in the resolution range 50.0–2.7 Å, with an $R(I)_{merge}$ of 4.8% (Table 1). Although CHP2 shows about 36% sequence identity with human CNB (PDB code 1aui; Kissinger *et al.*, 1995), molecular replacement using CNB as a search model with *MOLREP* (Vagin & Teplyakov, 1997) was unsuccessful. Further crystallization refinement and structural analysis by multi-wavelength anomalous dispersion methods using selenomethionine and also taking advantage of the presence of yttrium as an additive are in progress.

We thank the staff at beamlines BL44B2 and BL41XU, SPring-8 for data-collection support and Dr Tianxiang Pang for initial participation in this study. This work was supported by grant Nano-001 for Research on Advanced Medical Technology from the Ministry of Health, Labour and Welfare of Japan and Grant-in-Aid for Priority Areas 13142210 for Scientific Research from the Ministry of Education, Science and Culture of Japan. YBA was supported by a Japan Society for the Promotion of Science (JSPS) Postdoctoral Fellowship.

References

Barroso, M. R., Bernd, K. K., DeWitt, N. D., Chang, A., Mills, K. & Sztul, E. S. (1996). *J. Biol. Chem.* **271**, 10183–10187.
Bertrand, B., Wakabayashi, S., Ikeda, T., Pouysségur, J. & Shigekawa, M. (1994). *J. Biol. Chem.* **269**, 13703–13709.
Counillon, L. & Pouysségur, J. (2000). *J. Biol. Chem.* **275**, 1–4.
Kissinger, C. R., Parge, H. E., Knighton, D. R., Lewis, C. T., Pelletier, L. A., Tempczyk, A., Kalish, V. J., Tucker, K. D., Showalter, R. E., Moomaw, E. W., Gastinel, L. N., Habuka, N., Chen, X., Maldonado, F., Barker, J. E., Bacquet, R. & Villafranca, J. E. (1995). *Nature (London)*, **378**, 641–644.
Lin, X. & Barber, D. L. (1996). *Proc. Natl Acad. Sci. USA*, **93**, 12631–12636.
Lin, X., Sikkink, R. A., Rusnak, F. & Barber, D. L. (1999). *J. Biol. Chem.* **274**, 36125–36131.
Matsumoto, M., Miyake, Y., Nagita, M., Inoue, H., Shitakubo, D., Takemoto, K., Ohtsuka, C., Murakami, H., Nakamura, N. & Kanazawa, H. (2001). *J. Biochem.* **130**, 217–225.
Matthews, B. W. (1968). *J. Mol. Biol.* **33**, 491–497.
Nakamura, N., Miyake, Y., Matsushita, M., Tanaka, S., Inoue, H. & Kanazawa, H. (2002). *J. Biochem.* **132**, 483–491.
Orlowski, J. & Grinstein, S. (2004). *Pflugers Arch.* **447**, 549–565.
Otwinowski, Z. & Minor, W. (1997). *Methods Enzymol.* **276**, 307–326.
Pang, T., Hisamitsu, T., Mori, H., Shigekawa, M. & Wakabayashi, S. (2004). *Biochemistry*, **43**, 3628–3636.
Pang, T., Su, X., Wakabayashi, S. & Shigekawa, M. (2001). *J. Biol. Chem.* **276**, 17367–17372.
Pang, T., Wakabayashi, S. & Shigekawa, M. (2002). *J. Biol. Chem.* **277**, 43771–43777.
Putney, L. K., Denker, S. P. & Barber, D. L. (2002). *Annu. Rev. Pharmacol. Toxicol.* **42**, 527–552.
Timm, S., Titus, B., Bernd, K. & Barroso, M. (1999). *Mol. Biol. Cell*, **10**, 3473–3488.
Vagin, A. A. & Teplyakov, A. (1997). *J. Appl. Cryst.* **30**, 1022–1025.
Wakabayashi, S., Bertrand, B., Ikeda, T., Pouysségur, J. & Shigekawa, M. (1994). *J. Biol. Chem.* **269**, 13710–13715.
Wakabayashi, S., Shigekawa, M. & Pouyssegur, J. (1997). *Physiol. Rev.* **77**, 51–74.

Acta Physiol Scand 2005, 184, 187–193

Myocardial interstitial choline and glutamate levels during acute myocardial ischaemia and local ouabain administration

T. Kawada,[1] T. Yamazaki,[2] T. Akiyama,[2] T. Shishido,[1] H. Mori[2] and M. Sugimachi[1]

1 Department of Cardiovascular Dynamics, National Cardiovascular Center Research Institute, Osaka, Japan

2 Department of Cardiac Physiology, National Cardiovascular Center Research Institute, Osaka, Japan

Received 25 November 2004, accepted 16 March 2005
Correspondence: T. Kawada, Department of Cardiovascular Dynamics, National Cardiovascular Center Research Institute, 5-7-1 Fujishirodai, Suita, Osaka 565-8565, Japan.
E-mail: torukawa@res.ncvc.go.jp

Abstract

Aim: Noradrenaline (NA) uptake transporters are known to reverse their action during acute myocardial ischaemia and to contribute to ischaemia-induced myocardial interstitial NA release. By contrast, functional roles of choline and glutamate transporters during acute myocardial ischaemia remain to be investigated. Because both transporters are driven by the normal Na^+ gradient across the plasma membrane in a similar manner to NA transporters, the loss of Na^+ gradient would affect the transporter function, which would in turn alter myocardial interstitial choline and glutamate levels. The aim of the present study was to examine the effects of acute myocardial ischaemia and the inhibition of Na^+,K^+-ATPase on myocardial interstitial glutamate and choline levels.

Methods: In anaesthetized cats, we measured myocardial interstitial glutamate and choline levels while inducing acute myocardial ischaemia or inhibiting Na^+,K^+-ATPase by local administration of ouabain.

Results: The choline level was not changed significantly by ischaemia (from 0.93 ± 0.06 to 0.82 ± 0.13 μM, mean ± SE, $n = 6$) and was decreased slightly by ouabain (from 1.30 ± 0.06 to 1.05 ± 0.07 μM, $P < 0.05$, $n = 6$). The glutamate level was significantly increased from 9.5 ± 1.9 to 34.7 ± 6.1 μM by ischaemia ($P < 0.01$, $n = 6$) and from 8.9 ± 1.0 to 15.9 ± 2.3 μM by ouabain ($P < 0.05$, $n = 6$). Inhibition of glutamate transport by *trans*-L-pyrrolidine-2,4-dicarboxylate (*t*-PDC) suppressed ischaemia- and ouabain-induced glutamate release.

Conclusion: Myocardial interstitial choline level was not increased by acute myocardial ischaemia or by Na^+,K^+-ATPase inhibition. By contrast, myocardial interstitial glutamate level was increased by both interventions. The glutamate transporter contributed to glutamate release via retrograde transport.

Keywords acetylcholine, cardiac microdialysis, cats, coronary artery occlusion, myocardium, noradrenaline.

Acute myocardial ischaemia causes oxygen depletion and loss of ATP in the ischaemic region (Hearse 1979). Blockade of H^+-ATPase leads to noradrenaline (NA) leakage from storage vesicles and axoplasmic NA accumulation (Schömig *et al.* 1988). Intracellular acidosis causes Na^+ influx via Na^+/H^+ exchange. Inhibition of Na^+,K^+-ATPase activity reduces the Na^+ gradient across the plasma membrane. Because NA uptake transporters are driven by the normal Na^+ electrochemical gradient across the plasma membrane, axoplasmic NA accumulation and reduction of the Na^+ gradient cause reverse transport of NA from the intracellular space to the extracellular space (Schwartz 2000). Acute myocardial ischaemia evokes the myocardial interstitial NA release in the ischaemic region via retrograde NA transport, independently of efferent sympathetic nerve activity (Schömig *et al.* 1984, Yamazaki *et al.* 1996, Akiyama & Yamazaki 1999, Kawada *et al.* 2001a).

Similar to NA, choline and glutamate are taken up into cells by plasma membrane transporters driven by the Na^+ gradient (Schwartz 2000). We hypothesized that the loss of Na^+ gradient under ischaemic conditions would interfere with the transporter function, which would in turn alter myocardial interstitial choline and glutamate levels. Choline release has been suggested as an index of ischaemic degradation of the myocardial phospholipid bilayer in isolated, Tyrode solution-perfused rat hearts (Brühl *et al.* 2004). Glutamate can be a preferred myocardial fuel during ischaemia and may have protective effects on ischaemic myocardium (Arsenian 1998). Measuring myocardial interstitial levels of these molecules *in vivo* would contribute to understanding the pathophysiology of acute myocardial ischaemia. To test the hypothesis, we employed an *in vivo* cardiac microdialysis technique and measured myocardial interstitial choline and glutamate levels in anaesthetized cats (Akiyama *et al.* 1991, 1994, Yamazaki *et al.* 1997, Kawada *et al.* 2001b). Acute myocardial ischaemia inevitably affects systemic haemodynamics and perfusion of the heart. To minimize such haemodynamic effects, we also examined the effects of Na^+,K^+-ATPase inhibition on the myocardial interstitial choline and glutamate levels by locally administering ouabain through a dialysis probe (Yamazaki *et al.* 1999, Kawada *et al.* 2002). The results of the present study indicated that the myocardial interstitial choline level was not increased by acute myocardial ischaemia or by Na^+,K^+-ATPase inhibition. By contrast, the myocardial interstitial glutamate level was increased by both interventions. The glutamate transporter contributed to glutamate release via retrograde transport.

Materials and methods

Surgical preparation

Animal care was conducted in strict accordance with the *Guiding Principles for the Care and Use of Animals in the Field of Physiological Sciences* approved by the Physiological Society of Japan. Adult cats weighing 2.0–4.8 kg were anaesthetized via an intraperitoneal injection of pentobarbital sodium (30–35 mg kg^{-1}) and ventilated mechanically with room air mixed with oxygen. The depth of anaesthesia was maintained with a continuous intravenous infusion of pentobarbital sodium (1–2 mg kg^{-1} h^{-1}) through a catheter inserted via the right femoral vein. Mean systemic arterial pressure was monitored from a catheter inserted via the right femoral artery.

With the animal in the lateral position, the left fifth and sixth ribs were resected to expose the heart. When a coronary occlusion was necessary, a 3-0 silk suture was prepared around the left anterior descending coronary artery (LAD) just distal to the first diagonal branch. With a fine guiding needle, a dialysis probe was implanted into the left ventricular free wall perfused by the LAD. Heparin sodium (100 U kg^{-1} bolus injection followed by a maintenance dose of 50 U kg^{-1} h^{-1}) was administered intravenously to prevent blood coagulation. At the end of the experiment the experimental animals were killed by an overdose of pentobarbital sodium. We confirmed that the dialysis probe had been implanted within the left ventricular myocardium.

Dialysis technique

We designed a transverse dialysis probe (Akiyama *et al.* 1991, 1994). For measurements of small molecular compounds including ACh, choline, and glutamate, we used a dialysis fibre of 50 000 molecular weight cutoff (13 mm length, 310 μm OD, 200 μm ID; PAN-1200, Asahi Chemical, Osaka, Japan) with both ends glued to polyethylene tubes (20 cm length, 500 μm OD, 200 μm ID). The dialysis probe was perfused at a rate of 2 μL min^{-1} with Ringer solution. Each sample was collected in a microtube containing 3 μL of phosphate buffer (100 mM, pH 3.5). A cholinesterase inhibitor eserine (100 μM) was added to the perfusate to measure ACh. A preliminary examination indicated that whether the perfusate-contained eserine did not affect myocardial interstitial choline levels significantly. Dead space volume between the dialysis fibre and the sample microtube was identical for ACh, choline, and glutamate measurements, and the sampling was performed taking into account the time for dialysate to traverse the dead space volume.

The dialysate ACh and choline levels were measured directly by high-performance liquid chromatography with electrochemical detection. The absolute detection limits of ACh and choline, determined with a signal-to-noise ratio of 3, were 10 and 5 fmol per injection, respectively. The dialysate glutamate level was measured by kinetic enzymatic analysis with CMA 600. The absolute detection limit of glutamate was 1 μM per injection.

Protocols

All protocols were started from 2 h after implanting the dialysis probe. To examine changes in myocardial interstitial ACh and choline levels during acute myocardial ischaemia ($n = 6$), after collecting a 15-min baseline dialysate sample, we occluded the LAD for 60 min and obtained four consecutive 15-min dialysate samples. The full-length of the implanted dialysis fibre was located within the ischaemic area judged by discolouration of myocardium during the LAD occlusion. We then released the occlusion and collected a 15-min dialysate sample during reperfusion. To examine changes in myocardial ACh and choline levels in response to local ouabain administration ($n = 6$), after collecting a 15-min baseline dialysate sample, we replaced the perfusate with Ringer solution containing 100 μM ouabain and collected four consecutive 15-min dialysate samples.

In different groups of animals, myocardial interstitial glutamate levels were measured during acute myocardial ischaemia ($n = 6$) and during local administration of ouabain ($n = 6$). To elucidate the role of the glutamate transporter, we also examined the effects of glutamate transport inhibition by *trans*-L-pyrrolidine-2,4-dicarboxylate (*t*-PDC, 10 mM) on myocardial interstitial glutamate levels during acute myocardial ischaemia ($n = 7$) and local administration of ouabain ($n = 7$). *t*-PDC was locally administered through the dialysis probe to avoid systemic effects.

Statistical analysis

All data are presented as mean ± SE values. In each protocol, the effects of myocardial ischaemia or local ouabain administration were examined using one-way analysis of variance followed by Dunnett's test against the corresponding baseline level (Glantz 2002). The baseline as well as maximum glutamate levels with and without glutamate transport inhibition were compared by an unpaired *t*-test during acute myocardial ischaemia or during local ouabain administration (Glantz 2002). Differences were considered to be significant when $P < 0.05$.

Results

Figure 1a shows myocardial interstitial ACh level during acute myocardial ischaemia. The ACh level was increased by LAD occlusion, becoming approximately 15 times higher than the baseline level at 30–45 and 45–60 min of ischaemia. The ACh level decreased towards the baseline level upon reperfusion. Figure 1b illustrates myocardial interstitial choline level during acute myocardial ischaemia. The choline level did not change significantly throughout the ischaemic and reperfusion periods.

Figure 2a shows changes in myocardial interstitial ACh level during local administration of ouabain. The ACh level was increased by the inhibition of

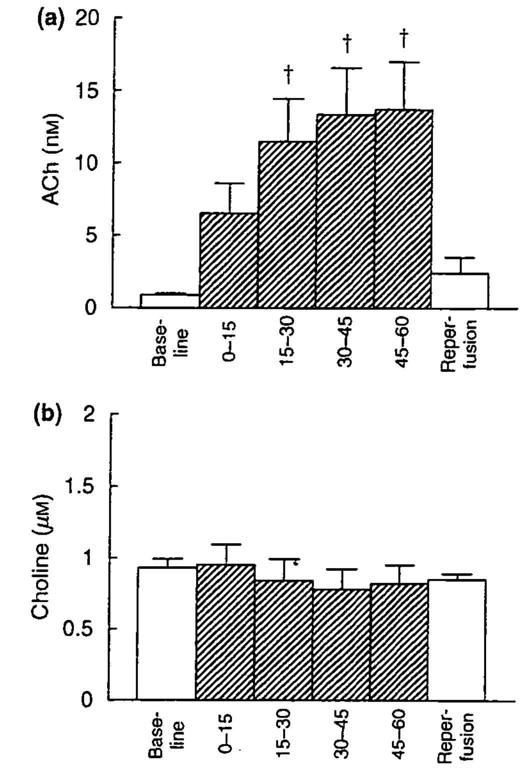

Figure 1 Changes in myocardial interstitial acetylcholine (ACh) level (a) and choline level (b) during coronary artery occlusion and reperfusion. Myocardial interstitial ACh level was significantly increased by acute myocardial ischaemia, while myocardial interstitial choline level was not changed. Data are mean ± SE. †$P < 0.01$ from baseline.

Na^+,K^+-ATPase, becoming approximately nine times higher than the baseline level at 15–30 min. The ACh level then decreased but remained significantly higher than the baseline level. Figure 2b illustrates the myocardial interstitial choline level during local administration of ouabain. The choline level was significantly lower at 0–15 and 45–60 min when compared with the baseline level.

Figure 3a shows changes in myocardial interstitial glutamate level during acute myocardial ischaemia. LAD occlusion increased the glutamate level to approximately 3.5 times higher than the baseline level at 0–15 min. Thereafter, the glutamate level was significantly higher than the baseline level throughout the ischaemic and reperfusion periods. Figure 3b illustrates the effects of glutamate transport inhibition on the ischaemia-induced glutamate release. The baseline glutamate level was significantly decreased by glutamate transport inhibition ($P < 0.05$). Although acute myocardial ischaemia and reperfusion significantly increased the glutamate level relative to the baseline level, the maximum glutamate level was attenuated to approximately one-fifth compared with that observed without glutamate transport inhibition ($P < 0.05$).

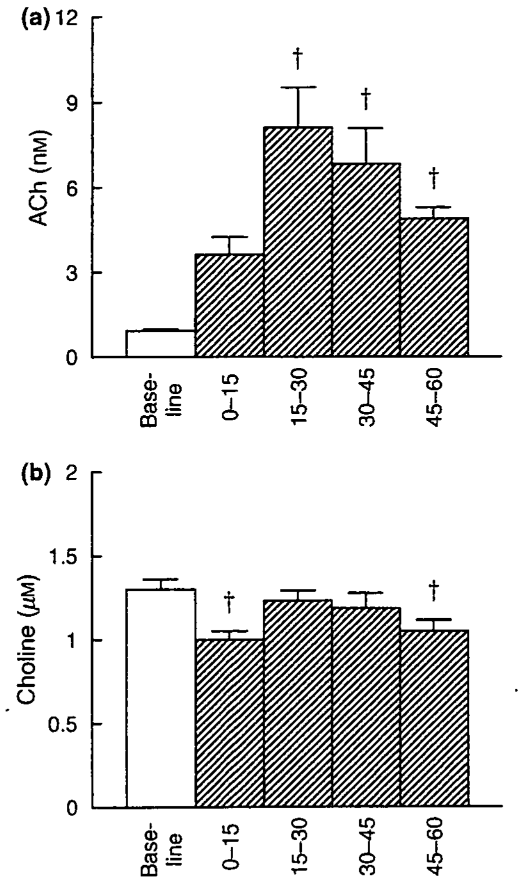

Figure 2 Changes in myocardial interstitial acetylcholine (ACh) level (a) and choline level (b) in response to the local administration of ouabain. Myocardial interstitial ACh level was significantly increased by ouabain. In contrast, myocardial interstitial choline level was decreased by ouabain. Data are mean ± SE. †$P < 0.01$ from baseline.

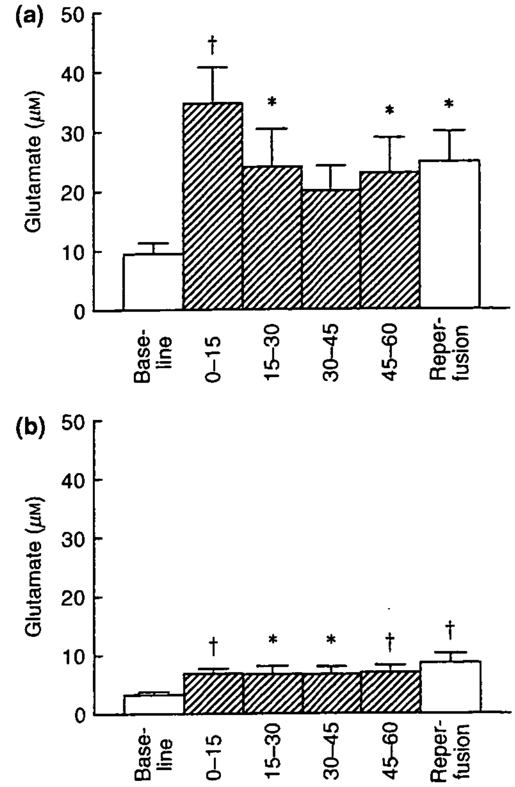

Figure 3 Changes in myocardial interstitial glutamate level during coronary artery occlusion and reperfusion without (a) and with (b) the inhibition of glutamate transporter. The glutamate level was significantly increased by acute myocardial ischaemia. The ischaemia-induced glutamate release was suppressed by the inhibition of glutamate transporter. Data are mean ± SE. †$P < 0.01$ and *$P < 0.05$ from baseline.

Figure 4a shows changes in myocardial interstitial glutamate level during the local administration of ouabain. Ouabain administration did not change the glutamate level at 0–15 min but increased the glutamate level thereafter. The glutamate level became approximately 1.8 times higher than the baseline level at 30–45 min. Figure 4b illustrates the effects of glutamate transport inhibition on ouabain-induced glutamate release. The baseline glutamate level was significantly decreased by the inhibition of glutamate transport ($P < 0.05$). Although ouabain administration increased the glutamate level relative to the baseline level, the maximum glutamate level was suppressed to approximately one-third of that observed without glutamate transport inhibition ($P < 0.05$).

Discussion

We have shown that acute myocardial ischaemia and local inhibition of Na^+,K^+-ATPase increased myocardial interstitial glutamate level but not choline level. Despite the similar Na^+ gradient dependency of corresponding transporters, myocardial interstitial glutamate and choline levels showed differential responses to the two interventions.

Changes in myocardial interstitial choline level

In the vagal nerve endings, ACh is hydrolysed to acetate and choline by acetylcholinesterase (Nicholls 1994). Choline is then taken up into the vagal nerve endings by the choline transporter driven by the Na^+ gradient. We hypothesized that loss of Na^+ gradient during acute myocardial ischaemia or local ouabain administration would increase the myocardial interstitial choline level by the interruption of choline uptake. Contrary to our hypothesis, acute myocardial ischaemia did not change myocardial interstitial choline level in the ischaemic region (Fig. 1b). Ouabain administration decreased the myocardial interstitial choline level at 0–15 and 45–60 min (Fig. 2b).

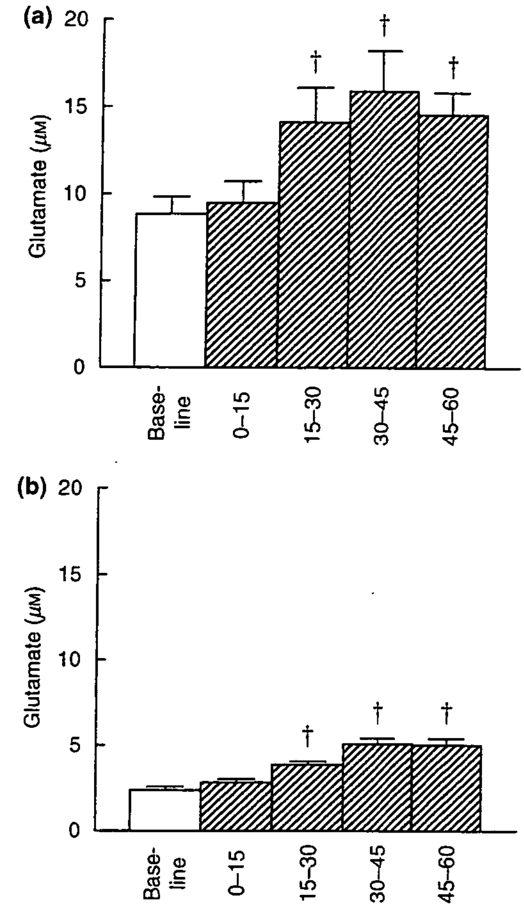

Figure 4 Changes in myocardial interstitial glutamate level in response to the local administration of ouabain without (a) and with (b) the inhibition of glutamate transporter. The glutamate level was significantly increased by ouabain administration. The ouabain-induced glutamate release was suppressed by the inhibition of glutamate transporter. Data are mean ± SE. †$P < 0.01$ from baseline.

Possible explanations for the absence of ischaemia- or ouabain-induced choline release are as follows. First, choline uptake is the rate-limiting step for ACh synthesis (Lockman & Allen 2002). Because choline in the intracellular space is rapidly consumed for ACh synthesis, the axoplasmic choline concentration might have been too low to evoke reverse transport by the choline transporter. Second, plasma choline concentration is stabilized by *de novo* choline synthesis from the catabolism of phosphatidylcholine found in cell membranes (Lockman & Allen 2002). Potential choline release may have been counterbalanced by the local stabilization mechanisms. Taking into account the recovery rate of the dialysis probe (approximately 30%), the myocardial interstitial choline concentration was 3–5 μM. Although the estimated concentration was lower than the highly regulated plasma choline concentration of approximately 10 μM, it was much higher than the ischaemia-induced maximum choline release (approximately 0.6 μM) in isolated rat hearts reported by Brühl *et al.* (2004). The present results suggest that myocardial interstitial choline level may not serve as an indicator of myocardial ischaemia in blood-perfused *in vivo* feline hearts.

By contrast with myocardial interstitial choline level, myocardial interstitial ACh level was increased both by acute myocardial ischaemia and by local administration of ouabain. Because ischaemia-induced ACh release was observed after vagal nerve transection in a previous study (Kawada *et al.* 2000), a Ca^{2+} channel-independent, regional release mechanism appears to be involved. Several reports have suggested that ouabain or ischaemia-induced intracellular Na^+ accumulation could elevate intracellular Ca^{2+} level via Na^+/Ca^{2+} exchange (Mochizuki & Jiang 1998, Li *et al.* 2000). The elevation of intracellular Ca^{2+} level may be associated with ACh release. Our previous study indicated that intracellular Ca^{2+} overload due to Ca^{2+} mobilization is responsible for the ACh release evoked by ischaemia (Kawada *et al.* 2000).

Changes in myocardial interstitial glutamate levels

Although the glutamate transporter family differs from the NA transporter family in that it requires countertransport of K^+ instead of cotransport of Cl^-, its primary driving force is the Na^+ gradient across the plasma membrane (Schwartz 2000). Therefore, interventions that reduce the Na^+ gradient are likely to cause reverse transport of glutamate, in a similar manner to the reverse transport of NA. Acute myocardial ischaemia increased the myocardial interstitial glutamate level (Fig. 3a) as consistent with previous reports (Kennergren *et al.* 1997, 1999, Bäckström *et al.* 2003, Song *et al.* 1996). Inhibition of Na^+,K^+-ATPase also induced myocardial interstitial glutamate release (Fig. 4a). Glutamate release during acute myocardial ischaemia and local ouabain administration was significantly attenuated by the inhibition of glutamate transport (Figs 3b and 4b), suggesting the involvement of reverse transport by the glutamate transporter. Glutamate plays a vital role in keeping nitrogen balance in cells as a common amino acid in transamination reactions. The high intra-to-extracellular concentration ratio of glutamate would contribute to the retrograde transport by the glutamate transporter during the loss of normal Na^+ gradient.

In the case of myocardial interstitial NA levels, local blockade of NA uptake increased baseline NA levels, suggesting the accumulation of NA spontaneously released into the synaptic cleft (Akiyama & Yamazaki 1999). We therefore predicted that the inhibition of glutamate transport would increase the baseline glutamate level. However, the inhibition of glutamate transport actually decreased the baseline glutamate level (Figs 3 and 4), suggesting that spontaneous glutamate release rather than glutamate uptake had occurred under baseline conditions. The insertion of a dialysis probe inevitably damages the myocardium. Although we waited for 2 h after implantation of the dialysis probe and the glutamate level declined with time, glutamate release from damaged myocardium may have continued. Notwithstanding this limitation, we were able to detect glutamate release in response to acute myocardial ischaemia and inhibition of Na^+,K^+-ATPase. Therefore, our interpretation that glutamate release was dependent on the reverse transport of glutamate transporter may be reasonable.

Supplementing the heart with glutamate has been shown to have beneficial effect on the recovery of contractile function in post-surgical patients (Arsenian 1998). The myocardial interstitial glutamate level remained increased during 15-min reperfusion whereas the myocardial interstitial ACh level returned towards the baseline level. Although the reason for different responses upon reperfusion was unanswered in the present study, the sustained increase in the glutamate level may have therapeutic effect on its own.

In conclusion, acute myocardial ischaemia and inhibition of Na^+,K^+-ATPase did not increase myocardial interstitial choline level despite a significant increase in myocardial interstitial ACh level. By contrast, both interventions significantly increased the myocardial interstitial glutamate level. The glutamate transporter contributed to myocardial interstitial glutamate release via retrograde transport.

This study was supported by Health and Labour Sciences Research Grant for Research on Advanced Medical Technology (H14-Nano-002) from the Ministry of Health Labour and Welfare of Japan, by Grant-in-Aid for Scientific Research (C-15590786) from the Ministry of Education, Science, Sports and Culture of Japan, and by the Program for Promotion of Fundamental Studies in Health Science of the Organization for Pharmaceutical Safety and Research from Pharmaceuticals and Medical Devices Agency (PMDA).

References

Akiyama, T. & Yamazaki, T. 1999. Norepinephrine release from cardiac sympathetic nerve endings in the in vivo ischemic region. *J Cardiovasc Pharmacol* 34(Suppl. 4), S11–S14.

Akiyama, T., Yamazaki, T. & Ninomiya, I. 1991. In vivo monitoring of myocardial interstitial norepinephrine by dialysis technique. *Am J Physiol Heart Circ Physiol* **261**, H1643–H1647.

Akiyama, T., Yamazaki, T. & Ninomiya, I. 1994. In vivo detection of endogenous acetylcholine release in cat ventricles. *Am J Physiol Heart Circ Physiol* 266, H854–H860.

Arsenian, M. 1998. Potential cardiovascular applications of glutamate, aspartate, and other amino acids. *Clin Cardiol* 21, 620–624.

Bäckström, T., Goiny, M., Lockowandt, U., Liska, J. & Franco-Cereceda, A. 2003. Cardiac outflow of amino acids and purines during myocardial ischemia and reperfusion. *J Appl Physiol* 94, 1122–1128.

Brühl, A., Hafner, G. & Löffelholz, K. 2004. Release of choline in the isolated heart, an indicator of ischemic phospholipid degradation and its protection by ischemic preconditioning: no evidence for a role of phospholipase D. *Life Sci* 75, 1609–1620.

Glantz, S.A. 2002. *Primer of Biostatistics*, 5th edn. McGraw-Hill, New York.

Hearse, D.J. 1979. Oxygen deprivation and early myocardial contractile failure: a reassessment of the possible role of adenosine triphosphate. *Am J Cardiol* 44, 1115–1121.

Kawada, T., Yamazaki, T., Akiyama, T. *et al.* 2000. Differential acetylcholine release mechanisms in the ischemic and non-ischemic myocardium. *J Mol Cell Cardiol* 32, 405–414.

Kawada, T., Yamazaki, T., Akiyama, T. *et al.* 2001a. Vagosympathetic interactions in ischemia-induced myocardial norepinephrine and acetylcholine release. *Am J Physiol Heart Circ Physiol* 280, H216–H221.

Kawada, T., Yamazaki, T., Akiyama, T. *et al.* 2001b. In vivo assessment of acetylcholine-releasing function at cardiac vagal nerve terminals. *Am J Physiol Heart Circ Physiol* **281**, H139–H145.

Kawada, T., Yamazaki, T., Akiyama, T. *et al.* 2002. Disruption of vagal efferent axon and nerve terminal function in the postischemic myocardium. *Am J Physiol Heart Circ Physiol* 283, H2687–H2691.

Kennergren, C., Nyström, B., Nyström, U. *et al.* 1997. In situ detection of myocardial infarction in pig by measurements of aspartate aminotransferase (ASAT) activity in the interstitial fluid. *Scand Cardiovasc J* 31, 343–349.

Kennergren, C., Mantovani, V., Lönnroth, P., Nyström, B., Berglin, E. & Hamberger, A. 1999. Extracellular amino acids as markers of myocardial ischemia during cardioplegic heart arrest. *Cardiology* 91, 31–40.

Li, S., Jiang, Q., Stys, P.K. 2000. Important role of reverse Na^+-Ca^{2+} exchange in spinal cord white matter injury at physiological temperature. *J Neurophysiol* 84, 1116–1119.

Lockman, P.R. & Allen, D.D. 2002. The transport of choline. *Drug Dev Ind Pharm* 28, 749–771.

Mochizuki, S. & Jiang, C. 1998. Na^+/Ca^{++} exchanger and myocardial ischemia/reperfusion. *Jpn Heart J* 39, 707–714.

Nicholls, D.G. 1994. *Proteins, Transmitters and Synapses*, pp. 186–199. Blackwell Science, London.

Schömig, A., Dart, A.M., Dietz, R., Mayer, E. & Kübler, W. 1984. Release of endogenous catecholamines in the ischemic myocardium of the rat. Part A: Locally mediated release. *Circ Res* 55, 689–701.

Schömig, A., Kurz, T., Richardt, G. & Schömig, E. 1988. Neuronal sodium homeostasis and axoplasmic amine concentration determine calcium-independent noradrenaline release in normoxic and ischemic rat heart. *Circ Res* 63, 214–226.

Schwartz, J.H. 2000. Neurotransmitters. In: E.R. Kandel, J.H. Schwartz & T.M. Jessell (eds) *Principles of Neural Science*, 4th edn, pp. 280–297. McGraw-Hill, New York.

Song, D., O'Regan, M.H. & Phillis, J.W. 1996. Release of the excitotoxic amino acids, glutamate and aspartate, from the isolated ischemic/anoxic rat heart. *Neurosci Lett* 220, 1–4.

Yamazaki, T., Akiyama, T., Kitagawa, H., Takauchi, Y. & Kawada, T. 1996. Elevation of either axoplasmic norepinephrine or sodium level induced release of norepinephrine from cardiac sympathetic nerve terminals. *Brain Res* 737, 343–346.

Yamazaki, T., Akiyama, T., Kitagawa, H., Takauchi, Y., Kawada, T. & Sunagawa, K. 1997. A new, concise dialysis approach to assessment of cardiac sympathetic nerve terminal abnormalities. *Am J Physiol Heart Circ Physiol* 272, H1182–H1187.

Yamazaki, T., Akiyama, T. & Kawada, T. 1999. Effects of ouabain on in situ cardiac sympathetic nerve endings. *Neurochem Int* 35, 439–445.

Am J Physiol Heart Circ Physiol 288: H1444–H1450, 2005.
First published November 11, 2004; doi:10.1152/ajpheart.00266.2004.

Adrenomedullin enhances therapeutic potency of bone marrow transplantation for myocardial infarction in rats

Takafumi Fujii,[1] Noritoshi Nagaya,[2,3] Takashi Iwase,[2] Shinsuke Murakami,[2] Yoshinori Miyahara,[1] Kazuhiro Nishigami,[3] Hatsue Ishibashi-Ueda,[5] Mikiyasu Shirai,[1] Takefumi Itoh,[2] Kozo Ishino,[6] Shunji Sano,[6] Kenji Kangawa,[4] and Hidezo Mori[1]

Departments of [1]Cardiac Physiology, [2]Regenerative Medicine and Tissue Engineering, [3]Internal Medicine, [4]Biochemistry, and [5]Pathology, National Cardiovascular Center, Osaka; and [6]Department of Cardiovascular Surgery, Okayama University Medical School, Okayama, Japan

Submitted 18 March 2004; accepted in final form 19 October 2004

Fujii, Takafumi, Noritoshi Nagaya, Takashi Iwase, Shinsuke Murakami, Yoshinori Miyahara, Kazuhiro Nishigami, Hatsue Ishibashi-Ueda, Mikiyasu Shirai, Takefumi Itoh, Kozo Ishino, Shunji Sano, Kenji Kangawa, and Hidezo Mori. Adrenomedullin enhances therapeutic potency of bone marrow transplantation for myocardial infarction in rats. *Am J Physiol Heart Circ Physiol* 288: H1444–H1450, 2005. First published November 11, 2004; doi: 10.1152/ajpheart.00266.2004.—Adrenomedullin (AM), a potent vasodilator, induces angiogenesis and inhibits cell apoptosis through the phosphatidylinositol 3-kinase/Akt pathway. Transplantation of bone marrow-derived mononuclear cells (MNC) induces angiogenesis. We investigated whether infusion of AM enhances the therapeutic potency of MNC transplantation in a rat model of myocardial infarction. Immediately after coronary ligation, bone marrow-derived MNC (5×10^6 cells) were injected into the ischemic myocardium, followed by subcutaneous administration of 0.05 $\mu g \cdot kg^{-1} \cdot min^{-1}$ AM (AM-MNC group) or saline (MNC group) for 3 days. Another two groups of rats received subcutaneous administration of AM alone (AM group) or saline (control group). Hemodynamic and histological analyses were performed 4 wk after treatment. Cardiac infarct size was significantly smaller in the MNC and AM groups than in the control group. A combination of AM infusion and MNC transplantation demonstrated a further decrease in infarct size. Left ventricular (LV) maximum change in pressure over time and LV fractional shortening were significantly improved only in the AM-MNC group. AM significantly increased capillary density in ischemic myocardium, suggesting the angiogenic potency of AM. AM infusion plus MNC transplantation demonstrated a further increase in capillary density compared with AM or MNC alone. Although MNC apoptosis was frequently observed 72 h after transplantation, AM markedly decreased the number of terminal deoxynucleotidyl transferase-mediated dUTP nick-end labeling-positive cells among the transplanted MNC. In conclusion, AM enhanced the angiogenic potency of MNC transplantation and improved cardiac function in rats with myocardial infarction. This beneficial effect may be mediated partly by the angiogenic property of AM itself and by its antiapoptotic effect on MNC.

angiogenesis; apoptosis; mononuclear cell

DESPITE THE RECENT REMARKABLE progress in medical and surgical treatment for ischemic heart disease, this disease remains a major cause of death worldwide (5). Bone marrow-derived mononuclear cells (MNC) contain various kinds of cell lineages and numerous cytokines that contribute to neovascularization (1, 15). In fact, autologous transplantation of bone marrow cells has been shown to enhance angiogenesis and improve cardiac function in an animal model of cardiac ischemia (6, 9, 10). Recent human studies have demonstrated beneficial effects of transplanted MNC in patients with ischemic heart disease (23, 25). However, some patients fail to respond to this cell therapy. Thus a novel therapeutic strategy to enhance the angiogenic property of MNC is desirable.

Adrenomedullin (AM) is a potent vasodilator peptide that was originally isolated from human pheochromocytoma (8). We have shown that infusion of AM has beneficial hemodynamic and renal effects in patients with heart failure (17). On the other hand, AM has been shown to activate the phosphatidylinositol 3-kinase (PI3-kinase)/Akt-dependent pathway in vascular endothelial cells, which is considered to regulate multiple critical steps in angiogenesis including endothelial cell proliferation, migration, and capillary-like formation (14, 22). In fact, we have shown that AM gene transfer induces therapeutic angiogenesis in a rabbit model of hindlimb ischemia via activation of Akt (24). These findings suggest that AM may play an important role in the regulation of vascular regeneration. In addition, AM has been shown to exert an antiapoptotic effect on a variety of cells including vascular endothelial cells (7, 20). Taking these findings together, combination therapy with MNC transplantation and AM infusion may have additional or synergetic effects on therapeutic angiogenesis for the treatment of ischemic heart disease.

Thus the purposes of this study were *1*) to investigate whether infusion of AM enhances the angiogenic potency of MNC transplantation in a rat model of myocardial infarction, and *2*) to investigate the effects of AM on survival and differentiation of the transplanted MNC to examine the underlying mechanisms of the effects induced by AM.

MATERIALS AND METHODS

Animal model. Myocardial infarction was produced in male Lewis rats weighing 200–220 g by left coronary ligation. In brief, after rats were anesthetized by intraperitoneal injection of pentobarbital sodium (30 mg/kg body wt), they were ventilated artificially. The heart was exposed via left thoracotomy, and the left coronary artery was ligated 2–3 mm from its origin between the pulmonary artery conus and the left atrium using a 6-0 proline suture. Finally, the heart was restored to its normal position, and the chest was closed. The Animal Care Committee of the National Cardiovascular Center approved this experimental protocol.

Address for reprint requests and other correspondence: N. Nagaya, Dept. of Regenerative Medicine and Tissue Engineering, National Cardiovascular Center Research Institute, 5-7-1 Fujishirodai, Suita, Osaka 565-8565, Japan (E-mail: nnagaya@ri.ncvc.go.jp).

The costs of publication of this article were defrayed in part by the payment of page charges. The article must therefore be hereby marked "*advertisement*" in accordance with 18 U.S.C. Section 1734 solely to indicate this fact.

Preparation of MNC. After Lewis rats were killed, bone marrow from the femur and tibia was collected and put in PBS. Marrow cells were loaded on a 1.077 gradient of Ficoll (Lymphoprep; Nycomed Pharma, Oslo, Norway) and centrifuged at 1,500 rpm for 20 min. The cells were then washed with 10 ml PBS to remove the Ficoll and centrifuged at 2,000 rpm for 10 min. The cells were finally suspended in PBS at a concentration of 5×10^6 cells in 50 μl PBS for transplantation. Fluorescence-activated cell sorting analysis demonstrated that 22 ± 1% of MNC were positive for lectin from ulex europaeus (UEA)-1 lectin (Sigma, St. Louis, MO).

MNC transplantation and AM infusion. Transplantation of bone marrow-derived MNC and/or 3-day infusion of AM was performed immediately after coronary ligation. MNC (5×10^6 cells in 50 μl PBS) were injected into the myocardium at five points in the border zone surrounding the infarct by using a 27-gauge needle. Recombinant human AM (0.05 $\mu g \cdot kg^{-1} \cdot min^{-1}$) was subcutaneously administered by using an osmotic minipump (model 2004; Alza, Palo Alto, CA) for 3 days. The pump was positioned in a pocket constructed in the subcutaneous tissue just below the subscapular region. For control, 5% glucose was infused in a similar manner in the rats receiving coronary ligation. This protocol resulted in the creation of four groups: *1*) AM infusion plus MNC transplantation (AM-MNC group, $n = 15$), *2*) vehicle infusion plus MNC transplantation (MNC group, $n = 14$), *3*) AM infusion plus PBS injection (AM group, $n = 14$), and *4*) vehicle infusion plus PBS injection (control group, $n = 13$).

Echocardiographic studies. Echocardiographic studies were performed 4 wk after surgery using a 7.5-MHz phased-array transducer (model HP SONOS 5500; Hewlett-Packard, Andover, MA). Rats were anesthetized by intraperitoneal injection of pentobarbital sodium (30 mg/kg body wt) as a supplement to maintain mild anesthesia. M-mode tracings were obtained at the level of the papillary muscles. Anterior and posterior end-diastolic wall thickness, left ventricular (LV) end-diastolic and end-systolic dimension, and LV fractional shortening were measured from three consecutive cardiac cycles by the American Society for Echocardiology leading-edge method (21).

Cardiac catheterization. Cardiac catheterization was performed 4 wk after surgery. Rats were anesthetized with intraperitoneal pentobarbital and placed on a heating pad to maintain body temperature at 37–38°C throughout the study. A 1.5 Fr micronanometer-tipped catheter was inserted in the right carotid artery for measurement of heart rate and mean arterial pressure. The catheter was then advanced into the LV for measurement of LV end-diastolic pressure and then replaced with a thermomicroprobe for measurements of cardiac output. These hemodynamic variables were measured with a pressure transducer (UFI, Morro Bay, CA) connected to a polygraph and recorded with a thermal recorder (model 7758 B system; Hewlett-Packard).

Infarct size measurement. After completion of hemodynamic measurements, the heart was arrested by an injection of 2 mmol KCl through the carotid artery, and the cardiac ventricles were excised. The size of myocardial infarction was determined by a previously described method (2). In brief, incisions were made in the LV so that the tissue could be pressed flat. The circumference of the entire flat LV and the visualized infarcted area, as judged from both the epicardial and endocardial sides, was outlined on a clear plastic sheet. The difference in weight between the two marked areas on the sheet was used to determine infarction size and was expressed as a percentage of LV surface area.

Histological analysis of microvessel density. LV myocardium was fixed in 10% formalin. Three cross sections of the LV, cut from apex to base, were obtained from individual rats for comparison among four groups ($n = 5$ each). They were embedded in paraffin and stained with Masson's trichrome for measurement of interstitial fibrosis. In other rats ($n = 5$ each), LV myocardium was embedded in optimum cutting temperature (OCT) compound (Sakura Finetechnical, Tokyo, Japan), snap frozen in liquid nitrogen, and cut into 5-μm-thick sections. Tissue sections were stained for alkaline phosphatase with an indoxyltetrazolium method to detect capillary endothelial cells ($n = 5$ in each group). The number of capillary vessels was counted in the peri-infarct area (a 1.0-mm band next to the scar) excluding scar region using a light microscope at a magnification of ×200. The numbers in five high-power fields in each rat were averaged and expressed as the number of capillary vessels. These morphometric studies were performed by two examiners who were blinded to treatment.

Detection of MNC apoptosis. To examine the antiapoptotic effect of AM on transplanted MNC, red fluorescence-labeled MNC were transplanted into ischemic myocardium in rats with ($n = 5$) and without ($n = 5$) AM infusion. Before implantation into the ischemic heart, suspended MNC were labeled with fluorescent dyes with a PKH26 (Red Fluorescent Cell Linker Kit; Sigma), as reported previously (13). AM was subcutaneously administered by using a minipump for 3 days. Rats were killed 72 h after MNC transplantation. The LV was enucleated, and muscle samples were embedded in OCT compound and snap frozen in liquid nitrogen for the detection of apoptosis. Serial sections of the heart were stained by terminal deoxynucleotidyl transferase-mediated dUTP nick-end labeling (TUNEL) for apoptosis using an in situ apoptosis detection kit (model S7111 Apoptag Fluorescein Kit; Intergen). Apoptosis of transplanted MNC was also evaluated by the detection of cleaved caspase-3-positive cells. In brief, the frozen tissue sections were incubated with anticleaved caspase-3 antibody (Cell Signaling), followed by incubation with FITC-conjugated IgG antibody (BD Pharmingen, San Diego, CA). The number of TUNEL/PKH26 double-positive cells and caspase-3/PKH26 double-positive cells was counted in 10 fields of each rat using a confocal microscopy (Fluoview model 500; Olympus, Tokyo, Japan).

The antiapoptotic effect of AM on MNC was also evaluated by in vitro TUNEL assay. MNC were plated on 12-well plates (1×10^6 cells per well) and cultured in serum-free medium for 24 h with control buffer, AM (1×10^{-7} M), or AM plus wortmannin, a PI3-kinase inhibitor (50 nM). Randomly selected microscopic fields ($n = 10$) were evaluated for calculating the ratio of TUNEL-positive cells to total cells.

Monitoring of implanted MNC in ischemic heart. Additional rats were used to examine whether transplanted MNC differentiate into endothelial cells, cardiomyocytes, vascular smooth muscle cells, or macrophages in the ischemic heart. PKH26 (red fluorescence)-labeled MNC were injected into the ischemic heart in rats with ($n = 8$) and without ($n = 8$) AM infusion. These subgroups of rats were killed 4 wk after coronary ligation. To identify vascular endothelial cells in vivo, FITC-labeled UEA-1 lectin was intravenously administered 30 min before the rats were killed ($n = 5$ in each group). The LV was enucleated, and muscle samples were then embedded in OCT compound, snap frozen in liquid nitrogen, and cut into sections. Sections were counterstained with 4′,6′-diamidino-2-phenylindole (DAPI) to detect nuclei. The number of DAPI/PKH26 double-positive cells and lectin-positive cells in the peri-infarct area was counted in 10 fields of each rat using a confocal microscopy. Frozen sections from other rats ($n = 3$ in each group) were incubated with mouse anticardiac troponin T (Novocastra, Newcastle, UK), anti-α-smooth muscle actin antibody (Dako, Copenhagen, Denmark), and anti-ED1 antibody (Serotec, Oxford, UK), followed by incubation with FITC-conjugated IgG antibody. In other rats (MNC group, $n = 5$; AM-MNC group, $n = 5$), the cardiac muscle from base to apex was transversely cut into 6-μm slices to calculate the number of transplanted MNC present within the heart 4 wk after transplantation. These morphometric studies were performed by two examiners who were blinded to treatment.

Statistical analysis. Numerical values were expressed as means ± SE. Comparisons of parameters among the four groups were performed by one-way ANOVA, followed by Newman-Keuls test for unpaired data. Comparisons of parameters between two groups were made by unpaired Student's *t*-test. A value of $P < 0.05$ was considered significant.

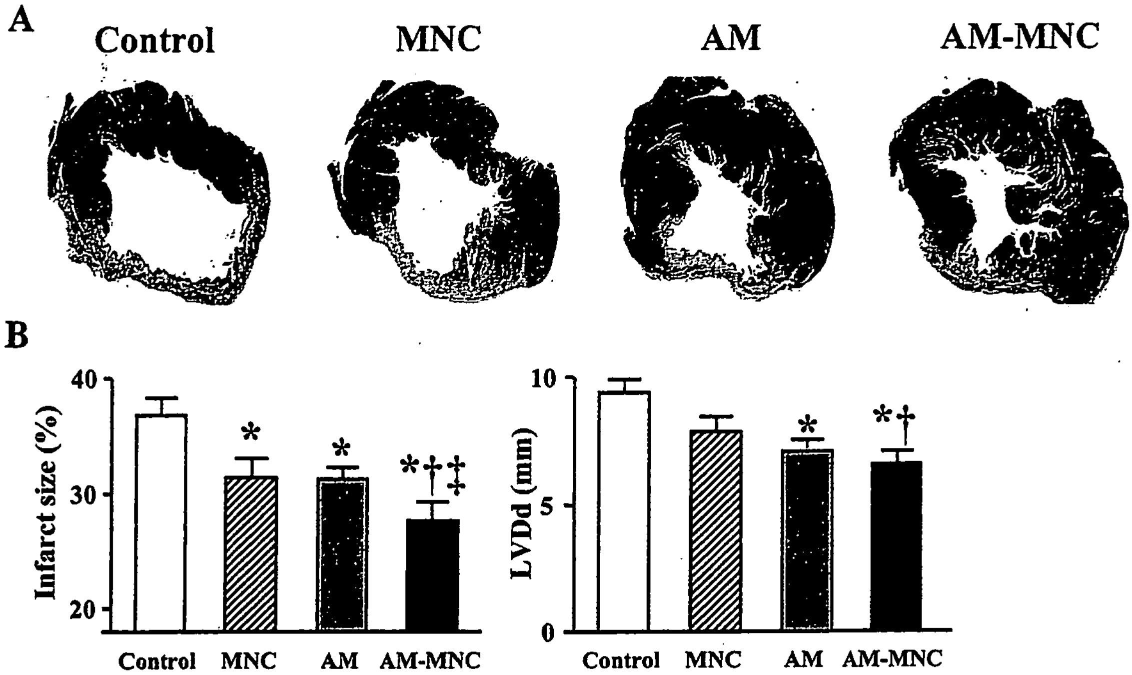

Fig. 1. *A*: representative examples of Masson trichrome-staining of transverse sections of left ventricular (LV) myocardium 4 wk after coronary ligation. *B*: quantitative analysis of infarct size and LV chamber size. Infarcted area and LV end-diastolic diameter (LVDd) of the adrenomedullin-mononuclear cell (AM-MNC) group were significantly smaller than those of the other groups. Values are means ± SE. **P* < 0.05 vs. control; †*P* < 0.05 vs. MNC; ‡*P* < 0.05 vs. AM.

RESULTS

Infarct size and ventricular weight. Moderate-to-large infarcts were observed in the control group after coronary ligation (Fig. 1). However, infarct size was smaller in the MNC, AM, and AM-MNC groups than in the control group. In particular, it was very small in the AM-MNC group. Quantitative analysis also demonstrated that cardiac infarct size in the AM-MNC group was smallest among the four groups. Right ventricular weight was significantly lower in the AM and AM-MNC groups than that in the control group (Table 1). LV weight did not significantly differ among the four groups.

Echocardiographic findings. LV diastolic dimension was smallest in the AM-MNC group, followed by the AM, MNC, and control groups (Fig. 1). LV fractional shortening in the AM-MNC group was also higher than that in the control, MNC, and AM groups (Table 2). Diastolic thickness of the anterior wall was significantly attenuated in the MNC, AM, and AM-MNC groups compared with the control group.

Hemodynamics. Cardiac output in the AM-MNC group was significantly higher than that in the control, MNC, and AM groups (Fig. 2). LV end-diastolic pressure in the MNC, AM, and AM-MNC groups was significantly lower than that in the control group. LV maximum change in pressure over time (dP/d*t*) in the MNC and AM-MNC group were significantly higher than that in the control group. Similarly, LV minimum dP/d*t* was significantly decreased only in the AM-MNC group.

Capillary density. Alkaline phosphatase staining of ischemic myocardium showed marked augmentation of neovascularization in the MNC, AM, and AM-MNC groups compared with the control group (Fig. 3*A*). Quantitative analysis demonstrated that capillary density was significantly higher in the AM-MNC group than in the MNC and AM groups (Fig. 3*B*). Cartilage, bone, or fat was not observed in the transplanted area. No tumor-like cells were seen.

Antiapoptotic effect of AM on MNC. Red fluorescence-labeled MNC were detected in each recipient heart 72 h after transplantation (Fig. 4). TUNEL-positive cells were frequently observed in the MNC group. In contrast, these apoptotic cells

Table 1. *Physiological profiles of four experimental groups*

	Control	MNC	AM	AM-MNC
Number	13	14	14	15
Body weight, g	274±3	285±5	287±3	305±4*
Heart rate, bpm	410±24	404±30	398±33	387±36
MAP, mmHg	101±11	104±13	103±9	116±14*
LV wt/body wt, g/kg	2.4±0.2	2.5±0.2	2.6±0.1	2.5±0.2
RV wt/body wt, g/kg	1.1±0.1	0.9±0.1	0.8±0.1*	0.7±0.1*

Values are means ± SE; number is number of rats in each group. Control group, myocardial infarction rats given vehicle; MNC group, those given mononuclear cells; AM, those given adrenomedullin; AM-MNC, those given AM and MNC; MAP, mean arterial pressure; LV, left ventricle; RV, right ventricle. **P* < 0.05 vs. control.

Table 2. *Echocardiographic findings*

	Control	MNC	AM	AM-MNC
LVDd, mm	9.9±0.2	8.3±0.3	7.3±0.2*	6.9±0.3*†
LVDs, mm	8.4±0.3	6.6±0.4	5.8±0.2*	5.1±0.2*
%FS, %	14±1	22±1*	21±1*	26±1*†‡
AWT diastole, mm	1.0±0.2	1.3±0.3*	1.3±0.3*	1.4±0.4*
PWT diastole, mm	1.5±0.5	2.2±0.4	2.1±0.4	2.2±0.4

Values are means ± SE. LVDd, LV diastolic dimension; LVDs, LV systolic dimension; %FS, LV fractional shortening; AWT, anterior wall thickness; PWT, posterior wall thickness. **P* < 0.05 vs. control; †*P* < 0.05 vs. MNC; ‡*P* < 0.05 vs. AM.

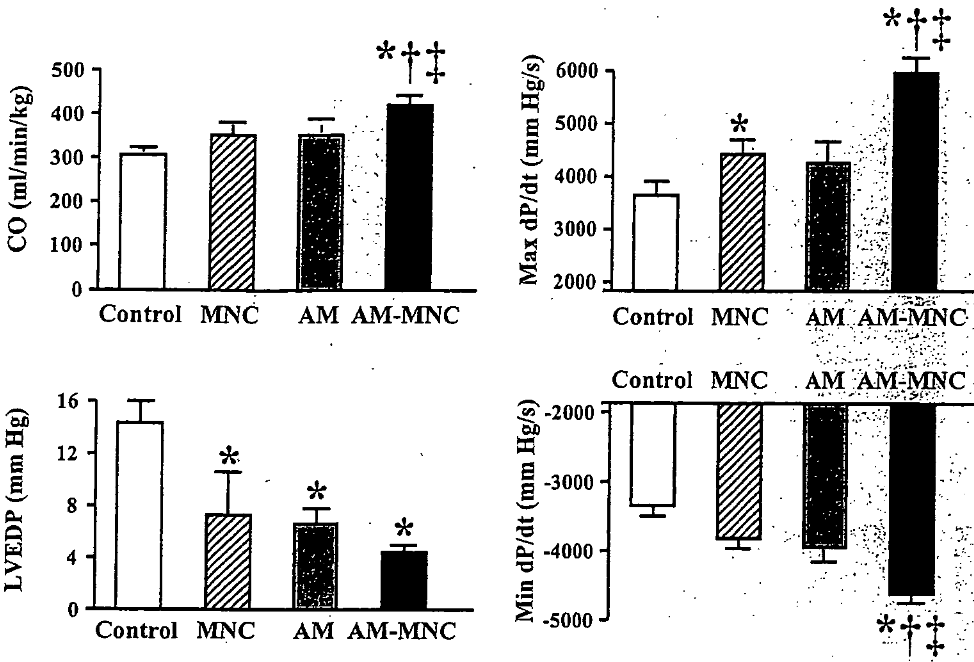

Fig. 2. Effects of AM infusion and MNC transplantation on hemodynamic parameters. CO, cardiac output; LVEDP, LV end-diastolic pressure; Max dP/d*t*, LV maximum change in pressure over time; Min dP/d*t*, LV minimum dP/d*t*. Values are means ± SE. **P* < 0.05 vs. control; †*P* < 0.05 vs. MNC; ‡*P* < 0.05 vs. AM.

were hardly detected in the AM-MNC group. Semiquantitative analysis demonstrated that the number of TUNEL-positive MNC was significantly lower in the AM-MNC group than in the MNC group. Similarly, the number of caspase-3-positive MNC was significantly lower in the AM-MNC group than in the MNC group. These results suggest that infusion of AM inhibits apoptosis of transplanted MNC.

In vitro, serum starvation induced MNC apoptosis. When incubated in the presence of AM (1×10^{-7} M), the percentage of TUNEL-positive cells decreased significantly (19 ± 1 to 9 ± 1%, $P < 0.05$). However, pretreatment with wortmannin, a PI3-kinase inhibitor, diminished the antiapoptotic effect of AM (17 ± 1%).

Differentiation of MNC into endothelial lineage. Four weeks after transplantation, fluorescence-labeled transplanted cells

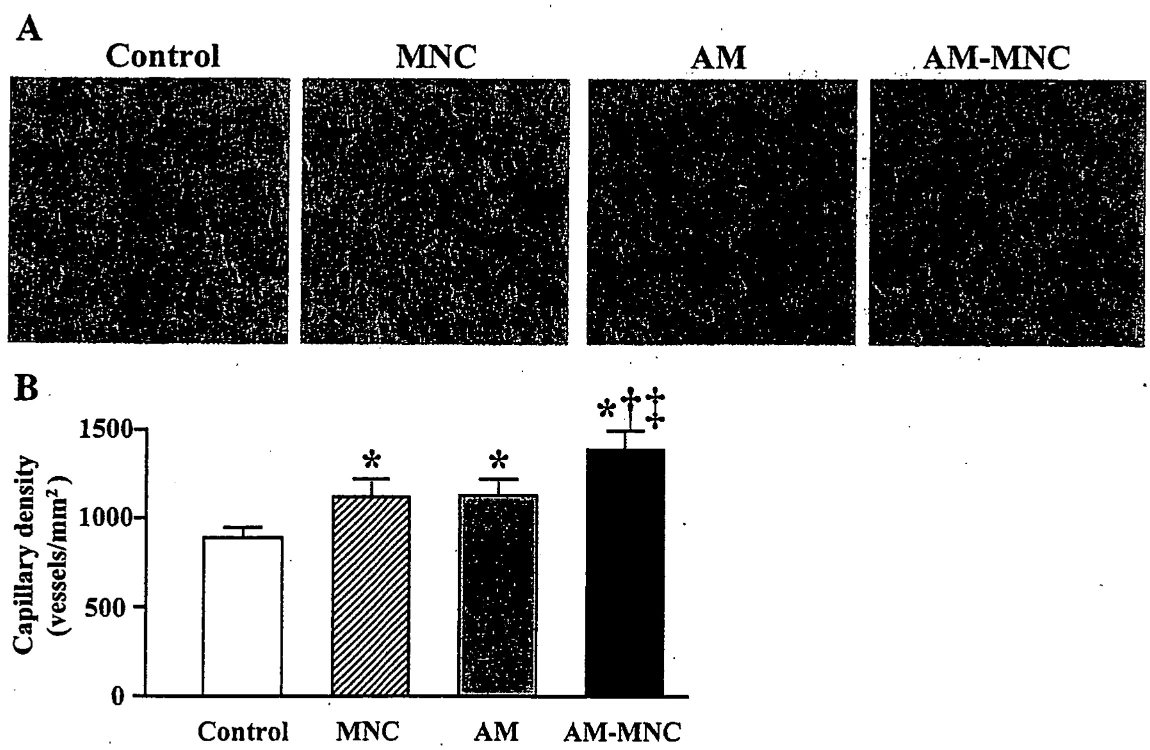

Fig. 3. *A*: representative examples of alkaline phosphatase staining in peri-infarct area. A combination of AM infusion and MNC transplantation markedly induced myocardial neovascularization. Magnification, ×200. *B*: quantitative analysis of capillary density in peri-infarct area. Capillary density in the AM-MNC group was significantly higher than that in the MNC and AM groups. Values are means ± SE. **P* < 0.05 vs. control; †*P* < 0.05 vs. MNC; ‡*P* < 0.05 vs. AM.

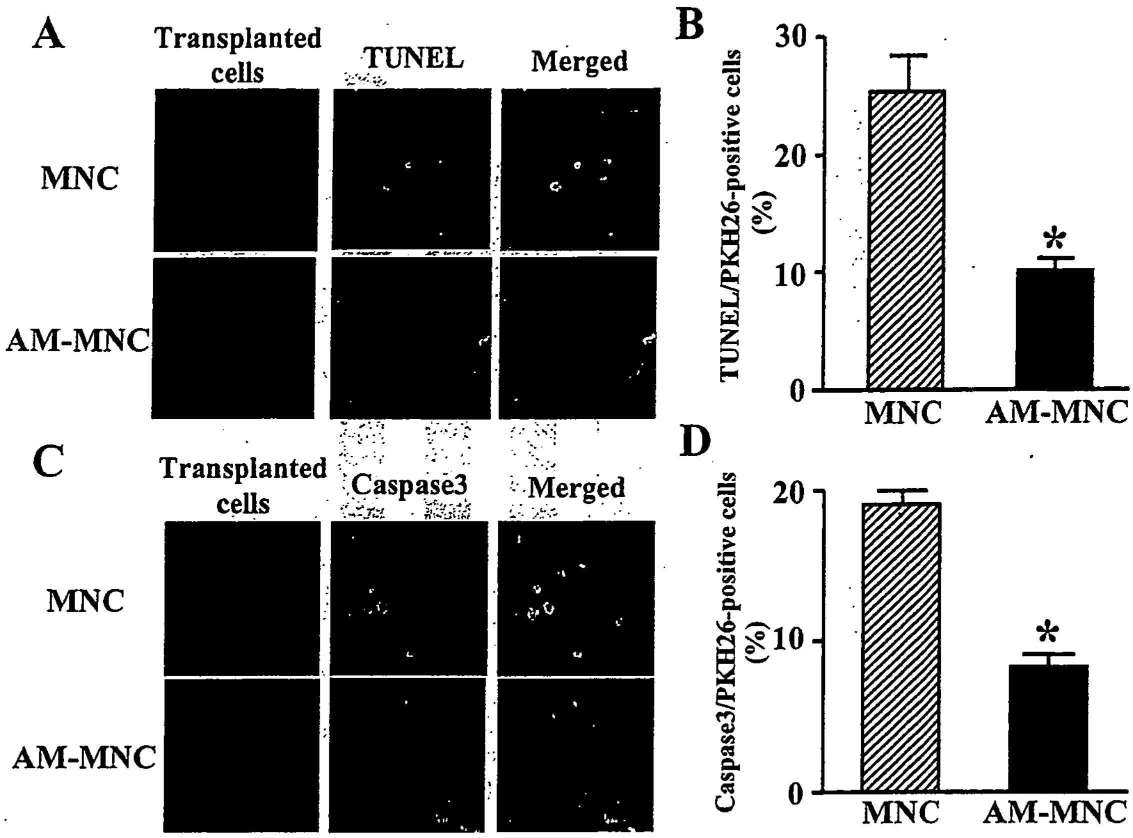

Fig. 4. Detection of transplanted cell apoptosis. *A*: representative photographs of terminal deoxynucleotidyl transferase-mediated dUTP nick end labeling (TUNEL) staining. Red fluorescence (PKH26) marks transplanted MNC; green fluorescence indicates TUNEL-positive cells. TUNEL-positive cells were frequently observed in the MNC group, whereas they were hardly detected in the AM-MNC group. Magnification, ×400. *B*: semiquantitative analysis of TUNEL-positive cells in the PKH26-positive (transplanted) cells. *C*: representative photographs of caspase-3 staining. Red fluorescence (PKH26) marks transplanted MNC; green fluorescence indicates caspase-3-positive cells. *D*: semiquantitative analysis of caspase-3-positive cells in the PKH26-positive cells. Values are means ± SE. **P* < 0.05 vs. control.

were more frequently observed in the AM-MNC group than in the MNC group (6.4 ± 0.4 to 3.1 ± 0.2%, $P < 0.05$). Moreover, some of the transplanted cells were positive for UEA-1 lectin in the AM-MNC group (Fig. 5*A*), suggesting differentiation of MNC into vascular endothelial cells. Semiquantitative analysis demonstrated that the number of DAPI/PKH26 double-positive cells (viable transplanted cells) was significantly higher in the AM-MNC group than in the MNC group (Fig. 5*B*). Moreover, the ratio of lectin-positive cells to DAPI/PKH26 double-positive cells was significantly higher in the AM-MNC group than in the MNC group. The ratio of DAPI/PKH26 double-positive cells to lectin-positive cells was small, but significantly higher in the AM-MNC group than in the MNC group (23.9 ± 0.9 to 17.2 ± 0.6%, $P < 0.01$). Transplanted MNC were negative for troponin T or α-smooth muscle actin-positive cells. Some of the transplanted MNC were positive for ED1, a marker of macrophage (data not shown).

DISCUSSION

In the present study, we demonstrated that *1*) infusion of AM enhanced the angiogenic potency of MNC in a rat model of acute myocardial infarction, resulting in decreased infarct size and improved cardiac function. We also demonstrated that *2*) AM induced angiogenesis and inhibited apoptosis of the transplanted MNC. Thus a combination of AM and MNC may have beneficial effects in rats with myocardial infarction, partly through the angiogenic potency of AM itself and through its antiapoptotic effect on MNC.

Bone marrow-derived MNC include a variety of stem and progenitor cells (1, 15, 19), some of which can differentiate into endothelial cells and secrete numerous cytokines and chemokines (6, 9, 10). Earlier studies (6, 9, 10, 23, 25) have shown that autologous bone marrow transplantation induces angiogenesis and improves LV function in animals and humans. However, some patients are refractory to this cell therapy. Thus an approach to augment the angiogenic potency of MNC transplantation is required.

The present study showed that MNC transplantation or AM infusion alone reduced infarct size. A combination of AM infusion and MNC transplantation resulted in further decreases in infarct size and LV chamber size. MNC transplantation or AM administration modestly improved LV function. On the other hand, a combination of MNC and AM significantly improved cardiac performance compared with MNC or AM alone, as indicated by increases in cardiac output, fractional shortening, and LV maximum dP/d*t*. Earlier studies (6, 9, 10) have reported that MNC transplantation induces therapeutic angiogenesis and preserves LV function through inhibition of cardiomyocyte apoptosis in animal models of myocardial infarction. We have shown that AM infusion during the acute phase of ischemia-reperfusion inhibits apoptosis of cardiomyocytes and produces hemodynamic improvement in an animal

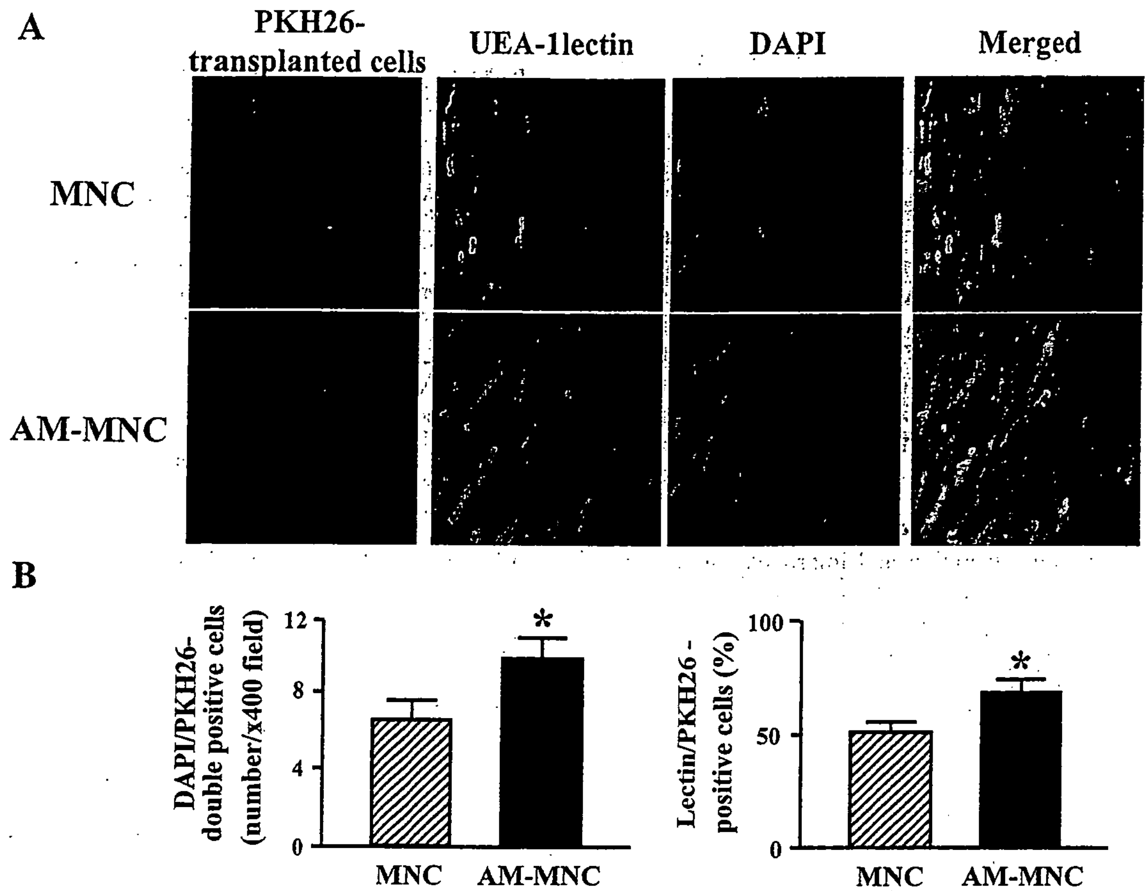

Fig. 5. *A*: representative examples of MNC differentiation into endothelial lineage. Red fluorescence (PKH26) marks transplanted cells; green fluorescence indicates ulex europaeus (UEA)-1 lectin, a marker for vascular endothelial cells. Most of the transplanted cells differentiated into endothelial cells in the AM-MNC group. Magnification, ×400. *B*: quantitative analysis of living transplanted cells and endothelial differentiation. The number of living cells after transplantation was significantly higher in the AM-MNC group than in the MNC group. The ratio of lectin-positive cells to living transplanted cells was significantly higher in the AM-MNC group than in the MNC group. Values are means ± SE. **P* < 0.05 vs. control. DAPI, 4′,6′-diamidino-2-phenylindole.

study (18). These findings suggest that the reduction of infarct size induced by this combination therapy may be attributable to additive cardioprotective effects of MNC and AM.

The present study showed that AM infusion significantly increased capillary density in ischemic myocardium. Furthermore, AM infusion plus MNC transplantation demonstrated a further increase in capillary density compared with AM or MNC alone. Contribution of transplanted MNC to neovascularization (the ratio of DAPI/PKH26 double-positive cells to lectin-positive cells) was significantly greater in the AM-MNC group than in the MNC group. A recent study (14) has reported that AM promotes proliferation and migration of human umbilical vein endothelial cells and enhances angiogenesis in a murine gel plug assay through the PI3-kinase/Akt pathway. We have also shown that intramuscular administration of AM DNA induces therapeutic angiogenesis in a rabbit model of chronic hindlimb ischemia via activation of Akt (24). These findings suggest that the beneficial effects of combination therapy using AM and MNC may be attributable, in part, to the angiogenic properties of AM itself. Thus it is possible that AM infusion and MNC transplantation induce additive effects on myocardial damage after myocardial infarction. However, it still remains unknown whether AM infusion plus MNC transplantation induces synergetic effects.

An earlier study has demonstrated that ischemia and mechanical stress induce apoptosis of transplanted cells in the early stage after MNC transplantation (9). These results raise the possibility that the angiogenic potency of MNC transplantation is attenuated by MNC apoptosis. Kim et al. (7) have demonstrated that AM inhibits apoptosis of endothelial cells through the PI3-kinase/Akt pathway in vitro. Activation of the PI3-kinase/Akt pathway has been shown to inhibit apoptosis of endothelial progenitor cells and enhance neovascularization (11). In the present study, AM infusion significantly inhibited MNC apoptosis in ischemic tissue. In vitro, we showed that the antiapoptotic effect of AM on MNC was mediated by activation of the PI3-kinase/Akt pathway. Thus AM may enhance the therapeutic potency of MNC transplantation through a direct action of AM on MNC survival. Moreover, immunohistological examination demonstrated that infusion of AM increased the number of lectin-positive (endothelial) cells in transplanted MNC. These findings raise the possibility that AM may enhance differentiation of MNC into the endothelial lineage. Thus AM may directly act on transplanted MNC, which may result in synergetic effects on the ischemic myocardium.

This study includes some study limitations. Although the labeling efficacy of PKH26 has been shown to persist for >8 wk without cell toxicity (3, 4), the used vital marker PKH26 may have some cell toxic effects and cell or membrane fusion can lead to labeling of neighboring cells in the target tissue. Second, the present study demonstrated that AM prolongs MNC survival through the PI3-kinase/Akt pathway and enhances neovascularization in a peri-infarcted area. However, further studies are necessary to examine the effect of AM on MNC differentiation into endothelial cells.

Autologous cell transplantation may be an alternative treatment for ischemic heart disease in the clinical setting. Because their use does not require immunosuppression, the clinical use of MNC for cellular cardiomyoplasty appears to be most advantageous. Administration of AM peptide is simple and relatively noninvasive. We and others (12, 16, 17) have reported the safety of AM infusion in humans. Thus combination therapy using AM infusion and MNC transplantation may be a new therapeutic strategy for the treatment of ischemic heart disease.

In conclusion, infusion of AM enhanced the angiogenic potency of MNC transplantation and improved cardiac function in rats with myocardial infarction. This beneficial effect may be mediated partly by the angiogenic property of AM itself and by its antiapoptotic effect on MNC. Thus combination therapy using AM infusion and MNC transplantation may be a new therapeutic strategy for the treatment of ischemic heart disease.

GRANTS

This work was supported by Ministry of Education, Culture, Sports, Science and Technology Grant-in-Aid for Scientific Research 13470154; Health and Labor Sciences Research Grants nano 001 and genome 005; Ministry of Health, Labor and Welfare Research Grant for Cardiovascular Disease H13C-1 and 16C-6; and grants from New Energy and Industrial Technology Development Organization and the Promotion of Fundamental Studies in Health Science of the Organization for Pharmaceutical Safety and Research of Japan.

REFERENCES

1. **Asahara T, Murohara T, Sullivan A, Silver M, van der Zee R, Li T, Witzenbichler B, Schatteman G, and Isner JM.** Isolation of putative progenitor endothelial cells for angiogenesis. *Science* 275: 964–967, 1997.
2. **Chien YW, Barbee RW, MacPhee AA, Frohlich ED, and Trippodo NC.** Increased ANF secretion after volume expansion is preserved in rats with heart failure. *Am J Physiol Regul Integr Comp Physiol* 254: R185–R191, 1988.
3. **Fox D, Kouris GJ, Blumofe KA, Heilizer TJ, Husak V, and Greisler HP.** Optimizing fluorescent labeling of endothelial cells for tracking during long-term studies of autologous transplantation. *J Surg Res* 86: 9–16, 1999.
4. **Gulbins H, Pritisanac A, Anderson I, Uhlig A, Goldemund A, Daebritz S, Meiser B, and Reichart B.** Myoblasts for survive 16 weeks after intracardiac transfer and start differentiation. *Thorac Cardiovasc Surg* 51: 295–300, 2003.
5. **Hennekens CH.** Increasing burden of cardiovascular disease: current knowledge and future directions for research on risk factors. *Circulation* 97: 1095–1102, 1998.
6. **Kamihata H, Matsubara H, Nishiue T, Fujiyama S, Tsutsumi Y, Ozono R, Masaki H, Mori Y, Iba O, Tateishi E, Kosaki A, Shintani S, Murohara T, Imaizumi T, and Iwasaka T.** Implantation of bone marrow mononuclear cells into ischemic myocardium enhances collateral perfusion and regional function via side supply of angioblasts, angiogenic ligands, and cytokines. *Circulation* 104: 1046–1052, 2001.
7. **Kim W, Moon SO, Sung MJ, Kim SH, Lee S, So JN, and Park SK.** Angiogenic role of adrenomedullin through activation of Akt, mitogen-activated protein kinase, and focal adhesion kinase in endothelial cells. *FASEB J* 17: 1937–1939, 2003.
8. **Kitamura K, Kangawa K, Kawamoto M, Ichiki Y, Nakamura S, Matsuo H, and Eto T.** Adrenomedullin: a novel hypotensive peptide isolated from human pheochromocytoma. *Biochem Biophys Res Commun* 192: 553–560, 1993.
9. **Kobayashi T, Hamano K, Li TS, Katoh T, Kobayashi S, Matsuzaki M, and Esato K.** Enhancement of angiogenesis by the implantation of self bone marrow cells in a rat ischemic heart model. *J Surg Res* 89: 189–195, 2000.
10. **Kocher AA, Schuster MD, Szabolcs MJ, Takuma S, Burkhoff D, Wang J, Homma S, Edwards NM, and Itescu S.** Neovascularization of ischemic myocardium by human bone-marrow-derived angioblasts prevents cardiomyocyte apoptosis, reduces remodeling and improves cardiac function. *Nat Med* 7: 430–436, 2001.
11. **Llevadot J, Murasawa S, Kureishi Y, Uchida S, Masuda H, Kawamoto A, Walsh K, Isner JM, and Asahara T.** HMG-CoA reductase inhibitor mobilizes bone marrow-derived endothelial progenitor cells. *J Clin Invest* 108: 399–405, 2001.
12. **McGregor DO, Troughton RW, Frampton C, Lynn KL, Yandle T, Richards AM, and Nicholls MG.** Hypotensive and natriuretic actions of adrenomedullin in subjects with chronic renal impairment. *Hypertension* 37: 1279–1284, 2001.
13. **Messina LM, Podrazik RM, Whitehill TA, Ekhterae D, Brothers TE, Wilson JM, Burkel WE, and Stanley JC.** Adhesion and incorporation of lacZ-transduced endothelial cells into the intact capillary wall in the rat. *Proc Natl Acad Sci USA* 89: 12018–12022, 1992.
14. **Miyashita K, Itoh H, Sawada N, Fukunaga Y, Sone M, Yamahara K, Yurugi-Kobayashi T, Park K, and Nakao K.** Adrenomedullin provokes endothelial Akt activation and promotes vascular regeneration both in vitro and in vivo. *FEBS Lett* 544: 86–92, 2003.
15. **Murohara T, Ikeda H, Duan J, Shintani S, Sasaki K, Eguchi H, Onitsuka I, Matsui K, and Imaizumi T.** Transplanted cord blood-derived endothelial precursor cells augment postnatal neovascularization. *J Clin Invest* 105: 1527–1536, 2000.
16. **Nagaya N, Kyotani S, Uematsu M, Ueno K, Oya H, Nakanishi N, Shirai M, Mori H, Miyatake K, and Kangawa K.** Effects of adrenomedullin inhalation on hemodynamics and exercise capacity in patients with idiopathic pulmonary hypertension. *Circulation* 109: 351–356, 2004.
17. **Nagaya N, Satoh T, Nishikimi T, Uematsu M, Furuichi S, Sakamaki F, Oya H, Kyotani S, Nakanishi N, Goto Y, Masuda Y, Miyatake K, and Kangawa K.** Hemodynamic, renal, and hormonal effects of adrenomedullin infusion in patients with congestive heart failure. *Circulation* 101: 498–503, 2000.
18. **Okumura H, Nagaya N, Itoh T, Okano I, Hino J, Mori K, Tsukamoto Y, Ishibashi-Ueda H, Miwa S, Tambara K, Toyokuni S, Yutani C, and Kangawa K.** Adrenomedullin infusion attenuates myocardial ischemia/reperfusion injury through the phosphatidylinositol 3-kinase/Akt-dependent pathway. *Circulation* 109: 242–248, 2004.
19. **Rafii S and Lyden D.** Therapeutic stem and progenitor cell transplantation for organ vascularization and regeneration. *Nat Med* 9: 702–712, 2003.
20. **Sata M, Kakoki M, Nagata D, Nishimatsu H, Suzuki E, Aoyagi T, Sugiura S, Kojima H, Nagano T, Kangawa K, Matsuo H, Omata M, Nagai R, and Hirata Y.** Adrenomedullin and nitric oxide inhibit human endothelial cell apoptosis via a cyclic GMP-independent mechanism. *Hypertension* 36: 83–88, 2000.
21. **Schiller NB, Shah PM, Crawford M, DeMaria A, Devereux R, Feigenbaum H, Gutgesell H, Reichek N, Sahn D, Schnittger I, Silverman NH, and Tajik AJ.** Recommendations for quantitation of the left ventricle by two-dimensional echocardiography. American Society of Echocardiography Committee on Standards, Subcommittee on Quantitation of Two-Dimensional Echocardiograms. *J Am Soc Echocardiogr* 2: 358–367, 1989.
22. **Shiojima I and Walsh K.** Role of Akt signaling in vascular homeostasis and angiogenesis. *Circ Res* 90: 1243–1250, 2002.
23. **Strauer BE, Brehm M, Zeus T, Kostering M, Hernandez A, Sorg RV, Kogler G, and Wernet P.** Repair of infarcted myocardium by autologous intracoronary mononuclear bone marrow cell transplantation in humans. *Circulation* 106: 1913–1918, 2002.
24. **Tokunaga N, Nagaya N, Shirai M, Tanaka E, Ishibashi-Ueda H, Harada-Shiba M, Kanda M, Ito T, Shimizu W, Tabata Y, Uematsu M, Nishigami K, Sano S, Kangawa K, and Mori H.** Adrenomedullin gene transfer induces therapeutic angiogenesis in a rabbit model of chronic hind limb ischemia: benefits of a novel nonviral vector, gelatin. *Circulation* 109: 526–531, 2004.
25. **Tse HF, Kwong YL, Chan JK, Lo G, Ho CL, and Lau CP.** Angiogenesis in ischaemic myocardium by intramyocardial autologous bone marrow mononuclear cell implantation. *Lancet* 361: 47–49, 2003.

Am J Physiol Heart Circ Physiol 289: H924–H930, 2005.
First published April 15, 2005; doi:10.1152/ajpheart.01207.2004.

Microdialysis separately monitors myocardial interstitial myoglobin during ischemia and reperfusion

Hirotoshi Kitagawa,[1] Toji Yamazaki,[2] Tsuyoshi Akiyama,[2] Masaru Sugimachi,[3] Kenji Sunagawa,[4] and Hidezo Mori[2]

[1]*Department of Anesthesiology, Shiga University of Medical Science, Otsu; Departments of* [2]*Cardiac Physiology and* [3]*Cardiovascular Dynamics, National Cardiovascular Center Research Institute, Suita; and* [4]*Department of Cardiovascular Medicine, Kyushu University Graduate School of Medical Sciences, Fukuoka, Japan*

Submitted 1 December 2004; accepted in final form 6 April 2005

Kitagawa, Hirotoshi, Toji Yamazaki, Tsuyoshi Akiyama, Masaru Sugimachi, Kenji Sunagawa, and Hidezo Mori. Microdialysis separately monitors myocardial interstitial myoglobin during ischemia and reperfusion. *Am J Physiol Heart Circ Physiol* 289: H924–H930, 2005. First published April 15, 2005; doi:10.1152/ajpheart.01207.2004.—Direct monitoring of myoglobin efflux during ischemia and reperfusion has been limited because of inherent sample collection problems in the ischemic region. Recently, the cardiac dialysis technique has offered a powerful method for monitoring myocardial interstitial levels of low-molecular-weight compounds in the cardiac ischemic region. In the present study, we extended the molecular target to high-molecular-weight compounds by use of microdialysis probes with a high-molecular-mass cutoff and monitored myocardial interstitial myoglobin levels. A dialysis probe was implanted in the left ventricular free wall in anesthetized rabbits. The main coronary artery was occluded for 60 or 120 min. We examined the effects of myocardial ischemia and reperfusion on myocardial interstitial myoglobin levels. Interstitial myoglobin increased within 15 min of ischemia and continued to increase during 120 min of ischemia, whereas blood myoglobin increased at 45 min of ischemia. Lactate and myoglobin in the interstitial space increased during the same period. At 60 min of ischemia, reperfusion markedly accelerated interstitial myoglobin release. The interstitial myoglobin level was fivefold higher at 0–15 min of reperfusion than at 60–75 min of coronary occlusion. The dialysis technique permits earlier detection of myoglobin release and separately monitors myoglobin release during ischemia and reperfusion. Myocardial interstitial myoglobin levels can serve as an index of myocardial injury evoked by ischemia or reperfusion.

infarction; interstitial space; membrane permeability

IT IS WELL KNOWN that certain proteins, including myoglobin, called serum cardiac markers, are released into the bloodstream in large quantities from necrotic cardiac muscle cells after myocardial infarction (20, 26, 43). However, because direct samples from the ischemic region are not readily obtainable, in situ studies on efflux of these proteins in the cardiac ischemic region have been limited (22). This problem of sample collection from the ischemic region remains unresolved. First, it is uncertain exactly when cardiac markers appear from injured myocardium. The appearance of cardiac markers indicates the turning point from reversible injury to irreversible damage (43). However, the first appearance of cardiac markers in the bloodstream is influenced by the slow transport of cardiac markers from the interstitial space into the bloodstream (20). Thus the detection of this appearance is of great value in understanding the pathophysiological events induced by myocardial ischemia. Second, recent experimental and clinical findings suggest that reperfusion itself seems to accelerate the release of cardiac markers (18, 37, 38). However, the extent to which reperfusion contributes to relative changes in their release is unclear. To determine myocardial injury evoked by reperfusion, more information is needed about the extent to which ischemia and reperfusion affect changes in the release of cardiac markers. Third, present methods used to measure infarct size require tissue analysis several hours after the ischemic event (8). Furthermore, histochemical analysis depends on the times of ischemia and reperfusion (23, 33). Concise, dissociated assessments of ischemia and reperfusion injury have been a frequent object of research.

In general, mobilization of cardiac markers from ischemic myocardium to the bloodstream has been divided into two different sequences: release from the myocardial cell to the interstitial space and transport from the interstitial space into the bloodstream (20). Therefore, if we examine the first process in in situ myocardium, we can discuss the pathophysiological changes during development of ischemic myocardial necrosis. However, little information is available on interstitial protein kinetics in the ischemic region (15). Examination of protein kinetics in the ischemic region has been limited to assessment of protein kinetics in the isolated Langendorff-perfused heart (28, 39). Recently, a cardiac dialysis technique has provided a powerful method for monitoring myocardial interstitial levels of low-molecular-weight compounds in the cardiac ischemic region (2, 6, 14, 31). Furthermore, this method is suitable for distinguishing between ischemia and reperfusion responses (32). By improving the microdialysis probes with a high-molecular-mass cutoff membrane, we have extended the molecular target to high-molecular-weight peptides and proteins and monitored myocardial interstitial protein levels.

In the present study, we chose myoglobin as one of the earliest biochemical markers in myocardial injury (4, 34). We applied the dialysis technique to the heart of anesthetized rabbits and investigated myocardial interstitial myoglobin levels during coronary occlusion and reperfusion. To address the above-mentioned issues, we compared the first appearance of myocardial interstitial myoglobin levels with that of low-molecular-weight metabolites (lactate and glycerol). Further-

Address for reprint requests and other correspondence: T. Yamazaki, Dept. of Cardiac Physiology, National Cardiovascular Center Research Institute, 5-7-1 Fujishirodai, Suita, Osaka 565-8565, Japan (E-mail: yamazaki@ri.ncvc.go.jp).

The costs of publication of this article were defrayed in part by the payment of page charges. The article must therefore be hereby marked "*advertisement*" in accordance with 18 U.S.C. Section 1734 solely to indicate this fact.

more, we compared the time course of myocardial interstitial myoglobin during reperfusion after ischemia with that of sustained ischemia and examined the changes in myoglobin release evoked by reperfusion. The results of the present study indicate that microdialysis is suitable for distinguishing between ischemia and reperfusion injury.

MATERIALS AND METHODS

Animal Preparation

The investigation conformed with the *Guide for the Care and Use of Laboratory Animals* published by the National Institutes of Health (NIH Publication No. 85-23, Revised 1996). All protocols were approved by the Animal Subjects Committee of the National Cardiovascular Center. Thirty adult male Japanese White rabbits (2.5–3.2 kg) were anesthetized with pentobarbital sodium (30–35 mg/kg iv). The level of anesthesia was maintained with a continuous intravenous infusion of pentobarbital sodium (1–2 $mg \cdot kg^{-1} \cdot h^{-1}$). The rabbits were intubated and ventilated with room air mixed with oxygen. Body temperature was maintained at ~39°C with a heating pad and lamp. Heart rate (HR), mean arterial pressure (MAP), and electrocardiogram were monitored and recorded continuously. Heparin sodium (200 IU/kg) was first administered intravenously and then maintained with a continuous infusion (5–10 $IU \cdot kg^{-1} \cdot h^{-1}$) to prevent blood coagulation. With the animal in the lateral position, the fifth or sixth rib on the left side was partially removed to expose the heart. A small incision was made in the pericardium, and the dialysis probe was implanted in the region perfused by the left circumflex coronary artery (LCX) of the left ventricular wall. A snare was placed around the main branch of the LCX to act as the occluder for later coronary occlusion. To ensure that the sampling area was in the ischemic region, we examined the color and motion of the ventricular wall during a brief occlusion and confirmed that the dialysis probe was correctly located. To avoid a preconditioning effect, the duration of occlusion was limited to a few seconds.

Dialysis Technique

We designed a handmade long transverse dialysis probe (1). One end of a polyethylene tube (25 cm long, 0.5 mm OD, 0.2 mm ID) was dilated with a 27-gauge needle (0.4 mm OD). Each end of the dialysis fiber (8 mm long, 0.215 mm OD, 0.175 mm ID, 300 Å pore size; Evaflux type 5A, Kuraray Medical) was inserted into the polyethylene tube and glued. A fine guiding needle (25 mm long, 0.51 mm OD, 0.25 mm ID) was used for implantation of the dialysis probes. A guiding needle was connected to the dialysis probe with a stainless steel rod (5 mm long, 0.25 mm OD). At a perfusion speed of 5 μl/min, the in vitro recovery rate (RR) of myoglobin was 15 ± 0.6% (number of dialysis probes = 3). In vitro RR was defined as follows: $RR = (C_{in} - C_{out})/C_{in}$, where C_{in} and C_{out} are the concentrations of myoglobin in the perfusate and in the dialysate, respectively (19). For monitoring myocardial interstitial lactate and glycerol levels, we used a conventional dialysis fiber (PAN-1200, Asahi Chemical Japan) to detect low-molecular-weight compounds (1).

Dialysis probes were perfused with Ringer solution (in mM: 147.0 NaCl, 4.0 KCl, and 2.25 $CaCl_2$) at 5 μl/min using a microinjection pump (model CMA/100, Carnegie Medicine). Figure 1 shows the time course of dialysate myoglobin levels collected at 1-h intervals over a 4-h period after probe implantation. Dialysate myoglobin rapidly decreased to 261 ± 56 ng/ml at 2 h after probe implantation. Thereafter, it gradually decreased, reaching an almost steady level of 222 ± 37 ng/ml 4 h after probe implantation. On the basis of the results of this experiment, in the subsequent protocol, we discarded the first 120-min collections of dialysate and measured the dialysate myoglobin level twice at 30-min intervals. When dialysate myoglobin levels reached the steady level, we started the experimental protocol.

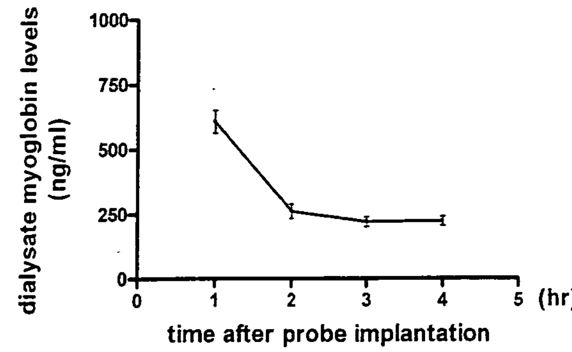

Fig. 1. Time course of dialysate myoglobin levels after probe implantation. Dialysate myoglobin levels decreased over the first 2 h and then reached an almost steady level. Values are means ± SE from 5 rabbits.

Sampling periods were 15 min (1 sampling volume = 75 μl) in control and during occlusion and reperfusion. Taking into consideration the dead space between the dialysis fiber and sample tube, we sampled the dialysate.

Dialysate myoglobin concentrations were measured as an index of myocardial interstitial myoglobin levels. Blood samples were obtained from the femoral artery. Using immunochemistry (Cardiac Reader, Roche Diagnostics), we measured the myoglobin levels (7). The detection limit of myoglobin was 30 ng/ml. The dialysate lactate and glycerol levels were measured by kinetic enzymatic analysis (CMA 600 analyzer, Carnegie Medicine) (30).

Experimental Protocols

After control sampling, we occluded the main branch of the LCX for 60 min and then released the occluder. We continuously sampled the dialysate from the ischemic region during 60 min of coronary occlusion and reperfusion.

Time course of dialysate lactate, glycerol, and myoglobin levels during myocardial ischemia. We compared the dialysate myoglobin levels with the blood myoglobin levels. After control sampling, we observed the time course of dialysate and blood myoglobin levels during 60 min of coronary occlusion. In addition, we measured simultaneously dialysate lactate and glycerol levels from the ischemic region in separate rabbits.

Time course of dialysate myoglobin levels during 60 min of reperfusion following 60 and 120 min of ischemia. Reperfusion modulates myocardial membrane damage and may accelerate dialysate myoglobin levels (18, 21, 37). We compared the time course of dialysate myoglobin during 60 min of reperfusion following 60 min of ischemia with that of 120 min of ischemia.

Time course of dialysate myoglobin levels during local administration of cyanide. To confirm whether the dialysate myoglobin level reflects myocardial damage evoked by ischemia or hypoxia, we tested the effect of local sodium cyanide (NaCN) administration on dialysate myoglobin levels. We collected a control dialysis sample and then replaced the perfusate with Ringer solution containing NaCN (30 mM), thereby locally administering NaCN for 60 min. We obtained four consecutive dialysate samples and measured the dialysate myoglobin levels.

At the end of each experiment, the rabbits were killed with an overdose of pentobarbital sodium, and the implant regions were checked to confirm that the dialysis probes had been implanted within the cardiac muscle.

Statistical Analysis

Dialysate lactate, glycerol, and myoglobin responses to coronary occlusion were statistically analyzed by one-way analysis of variance with repeated measures. When a statistically significant effect of